

Polarization Effects in Wavelength Converters based on Semiconductor Optical Amplifiers

Raul Martin Martin

Master of Science in Electronics

Submission date: July 2007

Supervisor: Dag Roar Hjelme, IET

Co-supervisor: Vegard Larsen Tuft, IET

Problem Description

The objective of this thesis is to study output orthogonality and nonlinear polarization rotations in the nodes of the OpMiGua network. In these nodes wavelength converters based on semiconductor optical amplifiers converts two orthogonal states of polarization to the desired wavelength. The study of the orthogonality between these two states of polarization in the output of the SOA is the main goal of this work.

Assignment given: 01. February 2007
Supervisor: Dag Roar Hjelme, IET

*A mis padres, Jesús y Maribel,
y a mi hermana Raquel, sin ellos
nunca hubiera llegado hasta aquí*

1. ABSTRACT

The OpMiGua network concept uses a model with two qualities of services travelling over two orthogonal states of polarization (SOP). A Mach-Zehnder interferometer based on semiconductor optical amplifiers (SOA-MZI) converts these SOP to the desired wavelength.

Following a brief introduction to semiconductor optical amplifiers, this paper gives an in depth analysis of how output orthogonality between these two SOPs, is affected by nonlinear polarization rotation in these devices. We consider that the polarized optical field can be decomposed into transverse electric and transverse magnetic components that have indirect interaction with each other. With this model we have obtained some results for output polarization angle of a semiconductor optical amplifier (SOA) in terms of the input polarization angle and furthermore investigate the relationship between these magnitudes and orthogonality.

CONTENTS

| | |
|---|----|
| ABSTRACT | 3 |
| 1. INTRODUCTION | 7 |
| 2. THEORY | 11 |
| 2.1 Cross-Phase Modulation | 11 |
| 2.2 Operation Principles in a SOA | 12 |
| 2.3 General Model SOA-MZI | 14 |
| 2.4 Analysis for TE and TM modes | 17 |
| 2.5 Model with Two Orthogonal signals | 20 |
| 3. RESULTS | 23 |
| 3.1 Basic Operation in a SOA | 23 |
| 3.2 TE and TM modes | 25 |
| 3.3 Signal with TE and TM components | 26 |
| 3.4 Orthogonality | 29 |
| 4. CONCLUSIONS | 37 |
| 5. REFERENCES | 39 |
| 6. ACKNOWLEDGEMENTS | 41 |
| 7. APPENDIX | 43 |

1. INTRODUCTION

Over the past few years, the great growth and continuous expansion of Internet, with the consistent increase of users and traffics, has led to high bandwidth requirements in the actual telecommunications networks. The current quality and capacity requirements, are higher and stricter than 10 years ago, because of that optical fiber has become very popular. Optical networks allow us satisfy the new and increasing needs of security and capacity transmission in demand by the companies, and probably in a not so far future, all of that with the greatest possible economy. The challenge of the future telecommunications networks points out to the only transmission of the high-capacity optical signals over long distance to effectively switching and managing data in optical domain. These functions, currently carried out in the electronic domain, are the main causes of the large bottleneck to the growth and scalability of Internet.

On the other hand, future networks are supposed to transport heterogeneous services both data transference, and multimedia and interactive applications. Therefore, each service needs specific requirements and processing, for example to guarantee a delay limit or a certain bandwidth..., being essential to be able to provide specific quality levels. In that environment to provide a Quality of Service (QoS) is a mandatory task. Using an appropriate network for it is necessary, a global, dynamic and easily scalable network. For that reason, in a few years, optical technology is going to be the perfect environment to develop the transport and treatment of all of these services and applications.

In current networks this need of quality of services must be satisfied, that is why services guarantees must be provided. Packet switched networks, which present Internet is based on, this is not a trivial task. Circuit switched networks can provide a dedicated path from transmitter to receiver without buffering and processing in intermediate nodes, thus there will be no buffer delay, jitter nor contention. On the other hand, these networks suffer from low granularity and lack the flexibility of statistically multiplexed packet switching.

Hybrid circuit and packet switched optical networks architectures combine the high resource utilization of packet switched networks with the low processing requirements of circuit switched networks. OpMiGua is one of these hybrid networks [1] [2]. OpMiGua (Optical packet switched Migration capable network with service Guarantees) is an hybrid optical network that combine advantages of the packet switched network with advantages of the circuit switched networks, being able to providing guaranteed service at the same time.

OpMiGua establish two different classes of service, applying a different kind of processing in the intermediate nodes for each one of them, one circuit-switched Guaranteed Service Traffic (GST) class and one packet-switched Statistically Multiplexed (SM) service class. OpMiGua consists of a wavelength routed optical network for transporting GST packets, and when the wavelength channel has vacant time periods, SM packets of a lower priority class of service are inserted,

exploiting channel capacity. Because of that, information processing faster is possible.

The two classes are time division multiplexed and transmitted on orthogonal states of polarization (SOP). To separate the two classes, we use polarization demultiplexing without complex packet header processing in intermediate nodes, with all the advantages that it means, like higher velocity and lower complexity. When a packet arrives to our network, it must be converted to the specific wavelength and assigned one of two orthogonal SOPs according to priority (figure 1). To convert these packets to the wavelength desired, we are going to use a Mach-Zender interferometer based on semiconductor optical amplifiers (SOA-MZI). It will convert incoming packets to the wavelength of a continuous wave (CW) probe beam switching the probe polarization between two orthogonal states [1], the converted packet is assigned a SOP according to its Quality of Service (QoS).

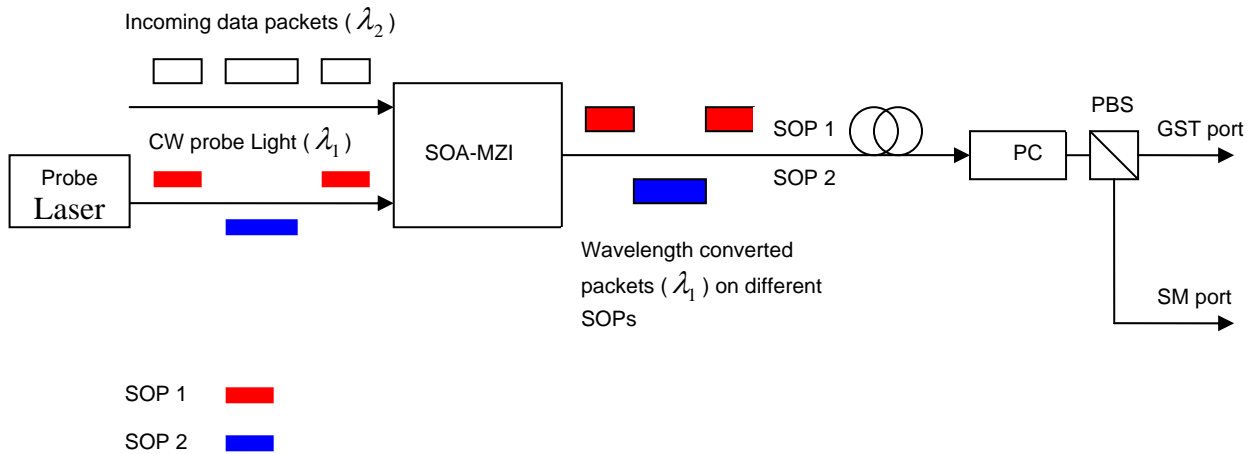


Figure 1: General Model. [2]

Demultiplexing of QoS classes is done by a polarization controller (PC) aligning the signal SOPs to the orthogonal axes of a polarization beam splitter (PBS). In case the two SOPs are not being perfectly orthogonal, some power from one SOP will couple into the wrong PBS output. So it is very important to make a detailed study of the sources of orthogonality degradation in optical communications networks. Polarization Dependent Loss (PDL) in components like multiplexers, filters, couplers...are known to degrade the orthogonality.

The main goal of this paper is to provide a deep analysis of the nonlinear polarisation rotation in wavelength converters previously commented. From these results we are going to study output orthogonality. This is a very important factor in OpMiGua networks. Polarization demultiplexing requires automatic polarization control for compensation of random polarization changes in the link and nodes. The

automatic polarization controller (APC) aligns the signal polarizations to the axes of a polarization beam splitter (PBS) which separates the two signals. Here the orthogonality between the two signals is very important in order to get the highest possible power.

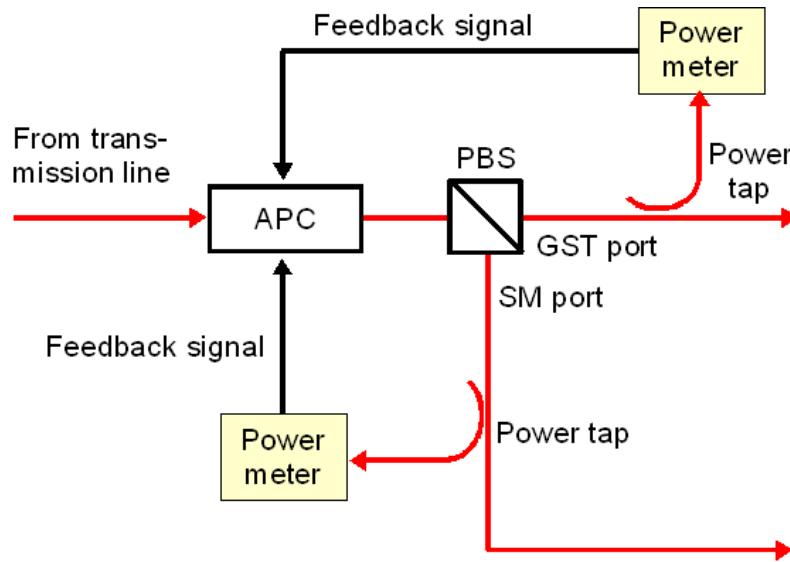


Figure 2: Polarization demultiplexing [1]

To carry out this study, in the first part of the report we are going to introduce theoretical concepts related to operation basic principles in these devices. Concepts like cross-phase modulation, wavelength conversion... will be studied. After it, the obtained results will be presented, starting by basic model of semiconductor optical amplifier, and following with the main model of the Mach-Zehnder interferometer based on semiconductor optical amplifier. In the final part of the report, we will get some conclusions about the most important factors that can affect output orthogonality. Matlab has been the mathematical tool used to do the simulations.

2. THEORY

It has been mentioned previously, that the main goal of this thesis is the study of orthogonality in the SOA, and how the different parameters in our scheme can affect this orthogonality, with the aim of configuring the best operation in our network.

We are working with the SOA in a MZI model, so the phase changes in the semiconductor optical amplifier are very important. To that purpose, first of all we must get a good understanding of the SOA operation, approaching to phase variations, and after it, we can introduce the SOA inside our scheme SOA-MZI to check the global behaviour.

2.1 Cross-Phase Modulation SOA CONVERTERS

The principle of the cross-phase modulation (XPM) scheme is based on the dependency of the refractive index on the carrier density in the active region of the SOA [3]. An incoming signal that depletes the carrier density will modulate the refractive index and thereby result in phase modulation of a CW signal coupled into the converter. The XPM scheme has the characteristic that the converted signal can be either inverted or non inverted regarding the input signal. In our case, we are going to work with noninverted signal.

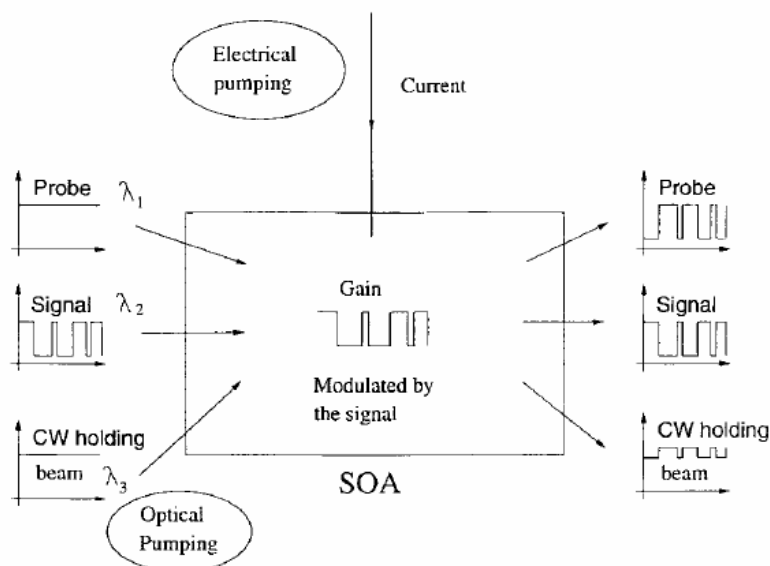


Figure 3: Conversion process in a SOA under electrical and optical pumping [4]

In this figure we can see the principle operation. A continuous-wave (CW) probe beam and a signal beam are injected into the SOA. The signal beam carrying the information at λ_2 modulates the gain of the SOA by depleting the carriers. It causes a change in the refractive index and a change in the phase of the optical beams. The probe beam amplitude and phase at wavelength λ_1 change with the modulated gain and refractive index. With low signal power values, the amplifier gain is unsaturated and the probe experiences a high value of gain, while with high signal power values, the amplifier gain is saturated and the probe experiences very little gain variation. The output probe signal amplitude is therefore modulated by the input signal.

The purpose of the third signal, CW holding, is to obtain a higher conversion speeds. It has been demonstrated in several papers [5], [6] that a higher photon density in the cavity can result in higher conversion speeds. In our model we are not going to use this third beam, because our main goal is not to calculate conversion speeds, therefore we can ignore the holding beam.

2.2 Operation Principles of an SOA

Our model is based on a thorough paper about semiconductor optical amplifiers [4]. We have taken into account all the characteristics of this model and after it we have done some approximations in order to do easier the simulations. These approximations are possible owing to the different goals we want to reach with our study. In this paper [4], the authors have approached their study towards to dynamics of the wavelength conversion process. Our work has been focused on static behaviour of the SOA, owing to we want to study different parameters. We have approximated equation 1 to zero, to study a time independent static model.

We have made a basic study of the SOA operation in different situations, finding the carrier density variation according to Input probe power, considering these results, we have calculated phase shift in SOA output. To make this analysis, we have used basic equation modelling SOAs, and simulations with Matlab have been developed. From [4] we get carrier density variation in a SOA:

$$\frac{dn}{dt} = \frac{J}{qd} - \frac{n}{T_s} - \sum_{w=1,2} \frac{g_{mw} I_w}{E_w} - g_{mp} S_t \quad (1)$$

where index w corresponds to the different optical input (signal and probe) beams, n is the carrier density, J is the drive current density, q is the electronic charge, and d is the active layer thickness. T_s is the carrier recombination life time, g_{mw} is the material gain for input beam w , and g_{mp} is its value at peak gain wavelength. S_t is the average amplified spontaneous emission. E_w is the photon energy and I_w represents the average light intensity for input beam inside segment of the SOA cavity.

Like we have commented before, we are doing a qualitative analysis; hence we will do into some approximations in order to make the study easier. It is the case of average amplified spontaneous emission, we are going to use $S_t=0$. Another approximation done is for the material gain, we can see the exact expression and the approximation here:

$$g_{mw} = a_1(n - n_0) - a_2(\lambda - \lambda_p)^2 \approx a_1(n - n_0) \quad (2)$$

being λ_p the gain peak wavelength. We are going to use this expression because we are interested on see how carrier density changes, the second term is a constant. Developing (1) for two beams and using the expression for material gain (2), we get the equation for carrier dynamics:

$$\frac{dn}{dt} = \frac{J}{qd} + a_1 n_0 \left(\frac{I_1}{E_1} + \frac{I_2}{E_2} \right) - n \left(\frac{1}{Ts} + \frac{a_1 I_1}{E_1} + \frac{a_1 I_2}{E_2} \right) - g_{mp} S_t \quad (3)$$

The nonlinear phase change, caused by carrier density induced changes in refractive index, is given by [4]

$$\Phi = \frac{2\pi L}{\lambda} \left(N_R + \Gamma n_p \frac{dN}{dn} \right) + \frac{2\pi L \Gamma (n_i - n_o)}{\lambda} \frac{dN}{dn} \quad (4)$$

L is the cavity length, n_0 is the transparency carrier concentration, λ is the beam wavelength, N_r is the guide refractive index and n_p is the value of carrier concentration for zero input power at the bias current used to define the peak gain wavelength. $\frac{dN}{dn}$ is the rate of change of active region refractive index with carrier concentration.

The device structure studied throughout this paper is a typical buried heterostructure SOA operating in the 1550 nm wavelength range. From [4] we get the next physical constants of the SOA:

| | | |
|----------------------|--------------------------------------|------------------------------------|
| D | 0.15 μm | Active layer Thickness |
| W | 1.2 μm | Active layer width |
| L | 500 μm | SOA length |
| n_0 | $1.1 \times 10^{18} \text{ cm}^{-3}$ | Transparency carrier density |
| $a_{1\text{TE}}$ | $2.5 \times 10^{-16} \text{ cm}^2$ | Material gain constant for TE mode |
| Γ_{TE} | 0.3 | Confinement factor for TE mode |

In [4] only a study for TE mode is done. From [7] we get confinement factor and material gain constant for TM mode:

| | | |
|---------------|------|------------------------------------|
| Γ_{TM} | 0.18 | Confinement factor for TM mode |
| a_{1TM} | 2.14 | Material gain constant for TM mode |
| N_{rTE} | 3.1 | Guide Refractive Index for TE mode |
| N_{rTM} | 2.9 | Guide Refractive Index for TM mode |

2.3 General Model SOA-MZI

Our SOA-MZI model is depicted in the next figure. This system is the basic structure for our wavelength converter. This model is based in a Mach-Zehnder interferometer (MZI) structure that incorporates a SOA in each arm of the MZI. The MZI has two inputs: the input data and a cw beam at the selected wavelength.

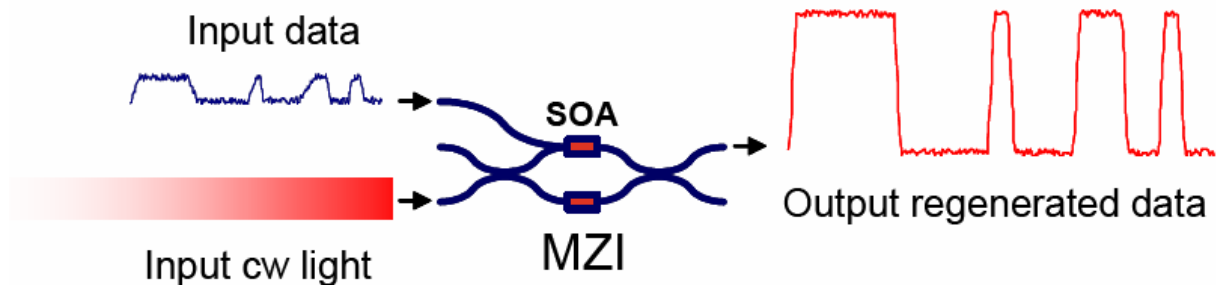


Figure 4: General model of the soa-mzi. [8]

Input optical data causes a gain reduction in one of the SOAs. This gain reduction produces an accompanying refractive index change that results in a phase change for the local cw light beam travelling through that SOA (the upper arm in Figure 4). This light beam on the upper arm of the MZI then optically interferes with the non-phase-shifted beam from the lower arm at the MZI output coupler.

Here we can see the expression for the output signal electric field:

$$\text{Output SOA-MZI} \rightarrow P_{out} = |E_{out}|^2$$

$$E_{out} = A_1 G e^{j\varphi_1} + A_2 G e^{j\varphi_2} = A_0 G e^{j\varphi_1} (1 + e^{j\Delta\varphi}) \quad (5)$$

We suppose A_0 is the input electric field amplitude for both signals, and G is the SOA gain.

φ_1 Output phase arm 1 of the soa-mzi

φ_2 Output phase arm 2 of the soa-mzi

being $\Delta\varphi = \varphi_2 - \varphi_1$

We have mentioned that XPM scheme has the characteristic that the converted signal can be either inverted or non inverted regarding the input signal. In this case we introduce in the second arm a pi phase shift to work with a noninverted signal.

In the case data signal is equal to '0' the phase difference between the two signals is $-\pi$, hence electric output field is zero:

$$\begin{aligned} \varphi_1 &= \varphi_{cw} \\ \varphi_2 &= \varphi_{cw} - \pi \end{aligned} \rightarrow \Delta\varphi = \varphi_2 - \varphi_1 = -\pi \rightarrow E_{output} = A_0 G e^{j\varphi_1} (1 + (-1)) = 0$$

For data signal = '1' we have:

$$\begin{aligned} \varphi_1 &= \varphi_{cw} \\ \varphi_2 &= \varphi_{cw} - \pi \end{aligned} \rightarrow \Delta\varphi = \varphi_2 - \varphi_1 = 0 \rightarrow E_{output} = 2A_0 G e^{j\varphi_1}$$

With the help of technical data from SOA manufacturer and our simulations is easy to set an specific rank of values for φ_1 to get the correct operation. The SOA-MZI must work in the right area of the MZI transmission curve.

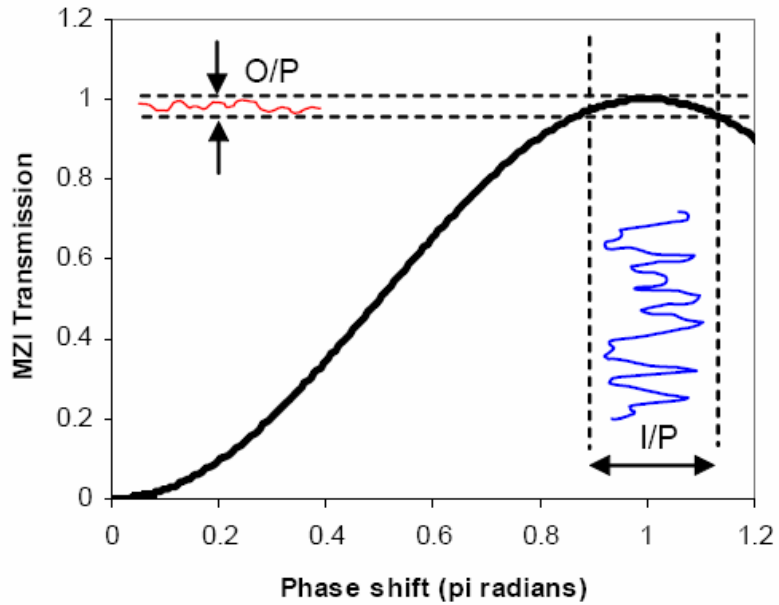


Figure 5: Relative transmission of the MZI upper output port as a function of the induced phase shift in the SOA. [8]

In this picture the transmission function for MZI is depicted. It means, if the induced phase shift is close to pi radians, the SOA operation will be optimum. We must try to get a phase shift as close as possible to pi radians.

2.4 Analysis for TE and TM modes

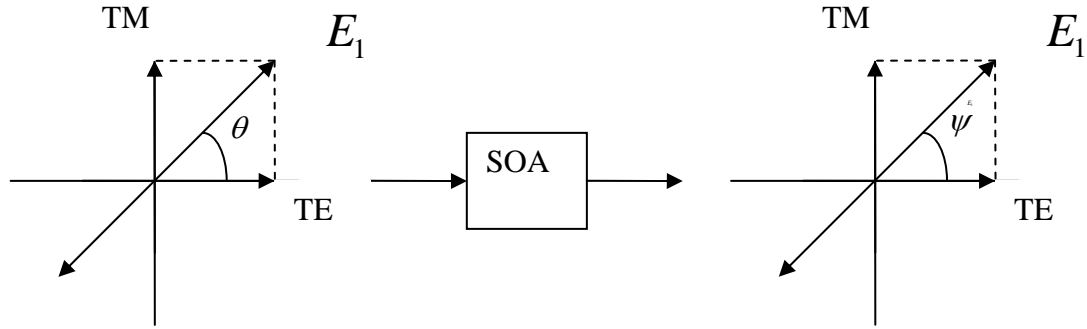


Figure 6: General transmission model with signal based on TE and TM components

To analyze correctly the SOA, first of all we must do a static analysis for the different cases with data signal equal to zero and data signal equal to one, without taking into consideration the change between both states. With this preliminary study, we can make a basic idea about SOA operation.

To develop a more quantitative understanding of the model showed in figure 6, we have used a model based on a propagating electric field, E , with two components aligned along the modes of the waveguide:

$$E = e^{j(\omega t - kz)} \left(E_{oTE} e^{j\Phi_{TE}} + E_{oTM} e^{j\Phi_{TM}} \right) \quad (6)$$

$$\begin{aligned} E_{oTE} &= \rho E \cos(\theta) u_{TE} \\ E_{oTM} &= E \sin(\theta) u_{TM} \end{aligned} \quad (7)$$

$E_{oTE(TM)}$ is the E component along the TE (TM) direction and its phase is $\Phi_{TE(TM)}$. ρ is the ratio of the single-pass gain in the TE mode to the single-pass gain in the TM mode, θ is the input angle and $u_{TE(TM)}$ is the unit vector along the horizontal (vertical) axis.

The phase change is different for the TE and TM components of the probe owing to the TE/TM asymmetry in both the confinement factors and effective guide refractive indices of the SOA. We have the equation (8) from [9]

$$\Phi = \frac{2\pi L}{\lambda} \left(N_{R(TE)/(TM)} + \Gamma_{(TE)/(TM)} n_p \frac{dN}{dn} \right) + \frac{2\pi L \Gamma_{(TE)/(TM)} (n_i - n_o)}{\lambda} \frac{dN}{dn} \quad (8)$$

From (8) we obtain the equation of the polarization ellipse where δ is the phase difference between the TE and TM components of the electric field [10]

$$\left(\frac{E_x}{E_{0TE}} \right)^2 + \left(\frac{E_y}{E_{0TM}} \right)^2 - 2 \frac{E_x E_y}{E_{0TE} E_{0TM}} \cos \delta = \sin^2 \delta \quad (9)$$

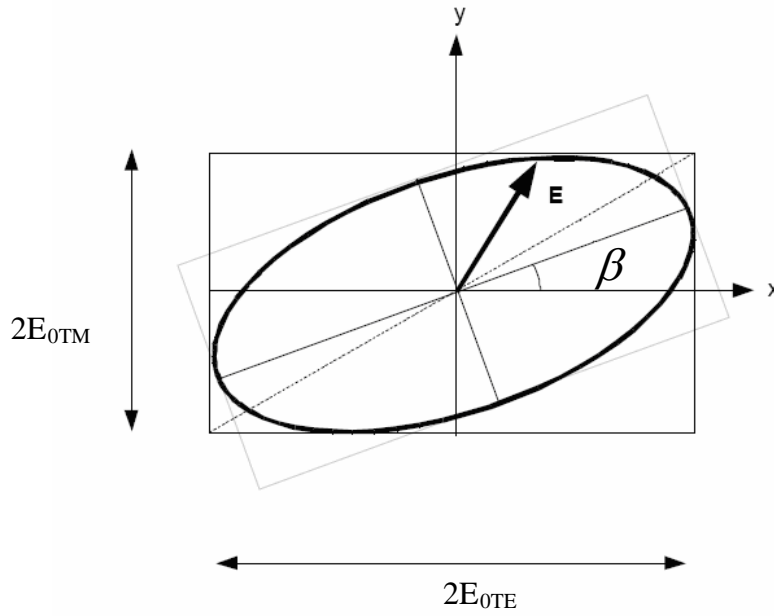


Figure 7: The polarization ellipse, [10].

This ellipse is rotated through an angle β regarding to x axis:

$$\tan(2\beta) = \frac{2E_{oTE} E_{oTM} \cos(\delta)}{E_{oTE}^2 - E_{oTM}^2} \quad (10)$$

δ is the phase difference between both electric fields. For that reason, a signal with two orthogonal components aligned along the modes of the waveguide undergoes a nonlinear polarization.

This nonlinear polarization rotation (NPR) is an important reason for this study, because our model is based on two orthogonal signals travelling along the SOA, and we want to check the most important factors that can modify this orthogonality. If the input probe polarization is not exactly coupled into TE or TM modes, there will be a rotation effect resulting from the SOA birefringence. Refractive indexes are different for both modes and therefore phase shift along SOA will be different, causing nonlinear polarization rotation.

At the same time, the difference between TE gain and TM gain will cause a change in the output polarization ellipticity, figure 8. The ellipticity is defined as the ratio of the length of the minor axis of the polarisation ellipse by the length of the major axis. An ellipticity of zero means that the polarisation is linear. An ellipticity of -1 corresponds to circular polarisation since both lengths are equal. The negative sign is a convention to define the left-handed rotation.

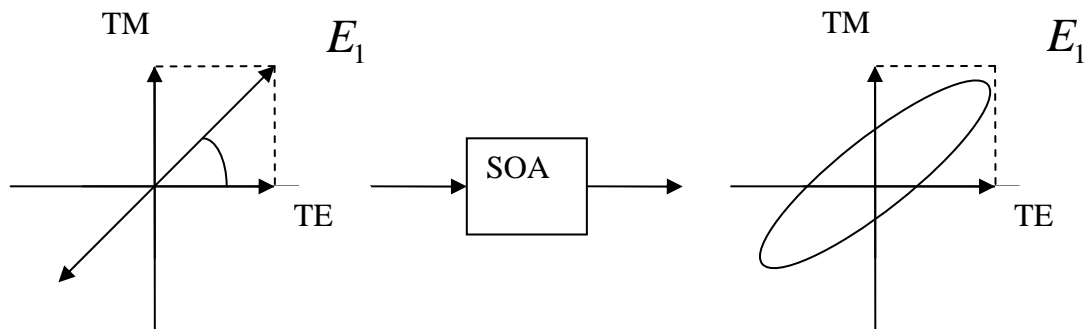


Figure 8: Input linear polarization / output elliptical polarization.

2.5 Two Orthogonal Signals

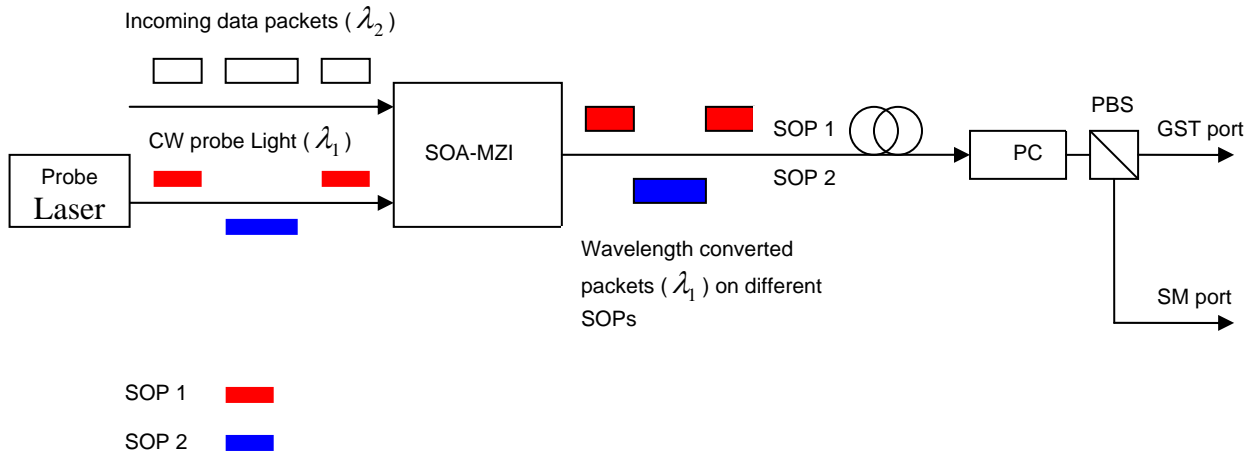


Figure 9: Basic Transmission and Reception Model. [2]

This is our general transmission model. We can see the SOA-MZI, the transmission line and the PC in the next node. As it was commented previously, the two classes are transmitted on orthogonal states of polarization. The SOP is used for all-optical class of service identification and separation by polarization demultiplexing, hence output orthogonality of these SOP is a very important factor.

It is known that Semiconductor Optical Amplifiers (SOAs) present nonlinearities that are used to achieve all-optical signal processing. In our model, these nonlinearities affect degrading the orthogonality between the two orthogonal modes. Our general model is based on the decomposition of the two orthogonal polarized optical fields into a transverse electric (TE) and a transverse magnetic (TM) component. These modes propagate “independently” through the SOA, although they have indirect interaction with each other.

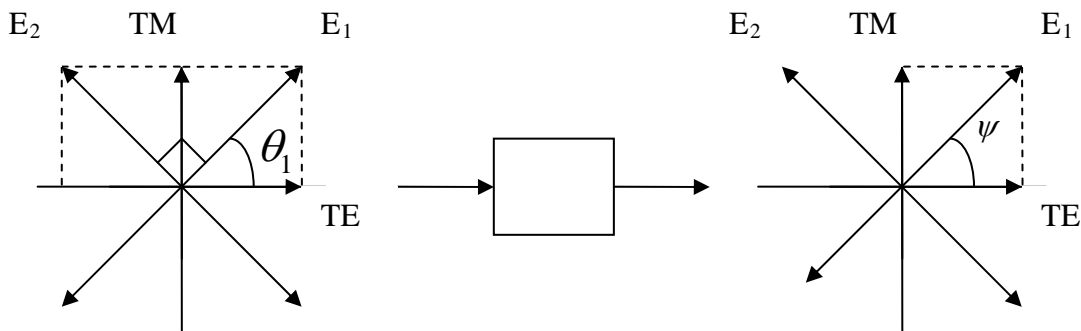


Figure 10: General model with two orthogonal signals

The two polarized optical fields in the SOA input are perfectly orthogonal

$$\begin{aligned} E_1 &= e^{j(\omega t - kz)} (E_{oTE1} e^{j\phi_{TE1}} + E_{oTM1} e^{j\phi_{TM1}}) \\ E_2 &= e^{j(\omega t - kz)} (E_{oTE2} e^{j\phi_{TE2}} + E_{oTM2} e^{j\phi_{TM2}}) \end{aligned} \quad (11)$$

where $E_{oTE(TM)1,2}$ is the E component along the TE (TM) direction for beam 1 and 2 respectively, and its phase is $\Phi_{TE(TM)1,2}$. $E_{oTE1,2}$ and $E_{oTM1,2}$ are expressed as:

$$\begin{aligned} |E_{oTE1}| &= \rho_1 E_1 \cos(\theta_1) \\ |E_{oTM1}| &= E_1 \sin(\theta_1) \end{aligned} \quad (12)$$

$$\begin{aligned} |E_{oTE2}| &= -\rho_2 E_2 \cos(\Pi - \theta_2) = -\rho_2 E_2 \cos\left(\frac{\Pi}{2} - \theta_1\right) \\ |E_{oTM2}| &= E_2 \sin(\Pi - \theta_2) = E_2 \sin\left(\frac{\Pi}{2} - \theta_1\right) \end{aligned} \quad (13)$$

ρ_1 and ρ_2 are the ratios of the single-pass gain in the TE mode to the single-pass gain in the TM mode for signal 1 and 2 respectively, and θ_1, θ_2 are the input polarization angles regarding to positive direction of the X - axis. Like in the previous section we can use (14):

$$\tan(2\psi) = \frac{2E_{oTE} E_{oTM} \cos(\delta)}{E_{oTE}^2 - E_{oTM}^2} \quad (14)$$

ψ is the output polarization angle and δ is the phase difference between TE and TM components.

$$\delta = \phi_{TM} - \phi_{TE} \quad (15)$$

In a polarization-sensitive SOA, the transverse electric (TE) and transverse magnetic (TM) components of the input signal experience different gains owing to the TE–TM asymmetry of the confinement factors, effective guide refractive indexes, and carrier distribution in an SOA. This internal birefringence increases in accordance with the light power through the SOA. Therefore, when a linearly polarized signal passes through the SOA, its state of polarization would rotate some angle toward the one principal axis of the amplifier structure that has greater gain [11]. For that reason each one of the two signals will experience a different polarization rotation, so output orthogonality will be affected.

The output vector for low power signal rotates more than the output vector for high power signal since the TE–TM gain ratio is higher for low power signals. This rotation is different depending on the angle of the input polarization regarding to main axis.

3. RESULTS

3.1 Basic operation of an SOA

First of all, we have obtained different graphics modelling basic behaviour of the SOA. In figure 11 and figure 12 we can see how the carrier density decrease with Input Optical Probe Power for the case of data signal equal to zero and data signal equal to one respectively.

This growing photon density, owing to higher probe power, causes an increasingly depletion of carrier density or gain of the amplifier. With low signal power values, the amplifier gain is unsaturated and the carrier density value is higher than with high signal power values.

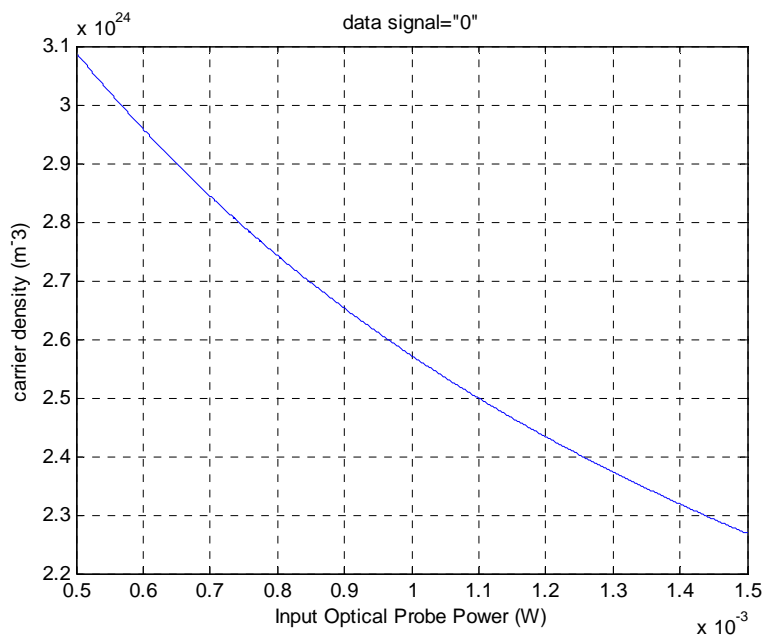


Figure 11: Carrier density vs. Input Optical Probe Power for data signal='0' (test1_zero.m)

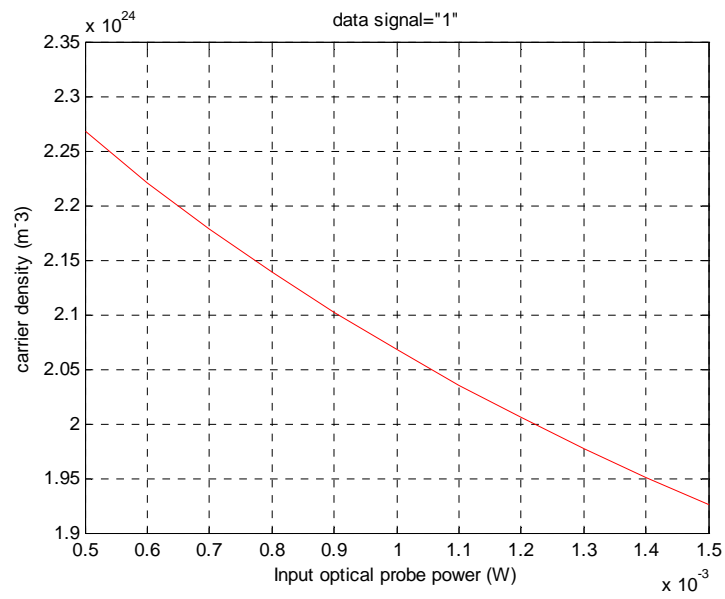


Figure 12: Carrier density vs. Input Optical Probe Power for data signal='1' (test1_one.m)

3.2 TE and TM modes

After we have seen the basic behaviour of the SOA, we have developed two matlab functions, to calculate the right value of Input probe power for the correct operation of the SOA-MZI. In the next two figures, the phase shift along the SOA has been depicted for TE and TM modes according to Input probe power. We can see the difference between phase shift for high power signal and low power signal.

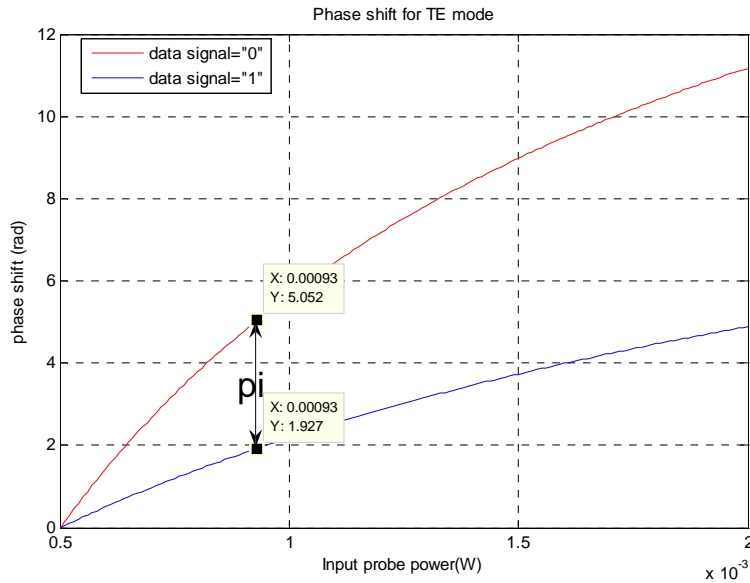


Figure 13: Variation of phase shift with Input probe signal power for TE mode (test2_TE.m)

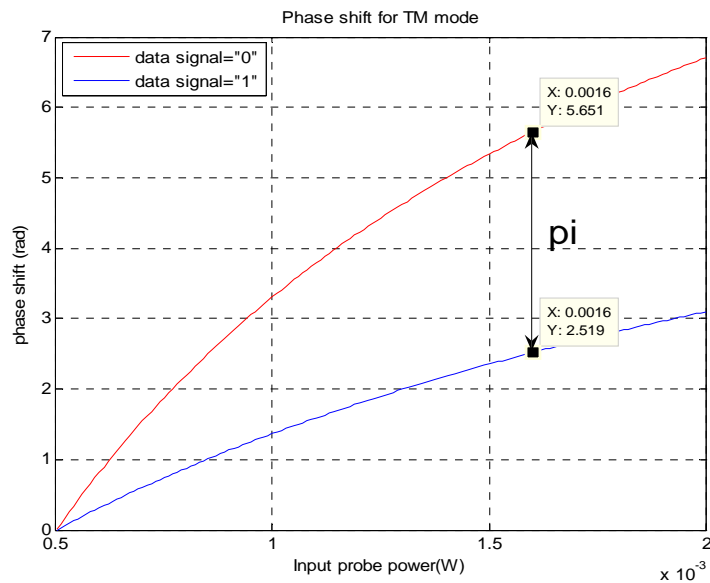


Figure 14: Variation of phase shift with Input probe signal power for TM mode (test2_TM.m)

According to the SOA's manufacturer catalogue, our model must work in the specified region for a correct operation of the SOA-MZI. It means the induced phase shift in the SOA must be around 0.9π radians and 1.1π radians.

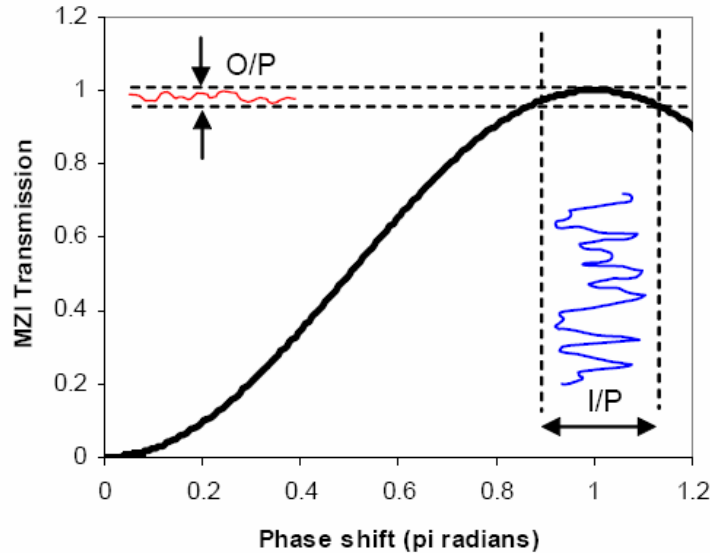


Figure 15: Relative transmission of the MZI upper output port as a function of the induced phase shift in the SOA. [8]

In our model, and having into account the π phase shift introduced in one arm of the interferometer, we can obtain the range of possible values for Input probe power. In the case of TE mode, a value around 0.93 mW will allow us to work in the desired region of the MZI Transmission graphic. In the case of TM mode, the value will be higher, around 1.6 mW . To calculate orthogonality in later sections, we will use the average value between optimal TE and optimal TM value.

3.3 Signal with TE and TM component

Now we are going to see the results for the principal case. We have a signal with TE and TM components and we want to see polarization rotations and orthogonality loss that is the main goal of this paper. First of all we must see how the output polarization angle ψ changes with input polarization angle θ , and with input power.

We have a signal with TE and TM component in the SOA input. It is going to undergo a rotation in function of its input polarization angle and its input power. We have developed a Matlab function, test3.m, to check how ψ changes when θ varies. With the equations (12), (13) and (14), we can see the relation between these two angles.

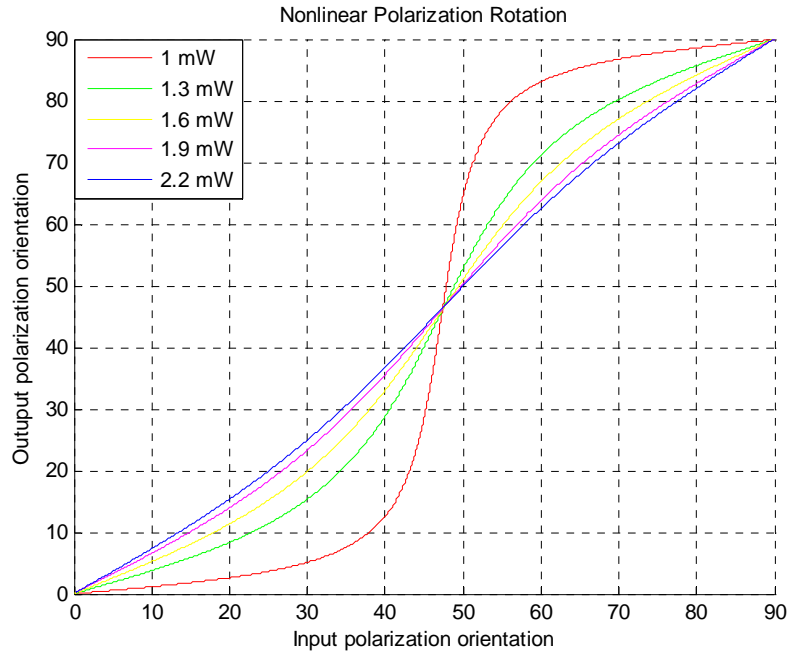


Figure 16: Variation of Output polarization angle with Input polarization angle for different power levels (test3.m)

Analysing this graphic some results can be drawn. For example, at an input orientation, θ , of 45° , there will be the same light injected into the TE and the TM mode, and the output orientation ψ is of 28° , hence TE gain must be greater than the TM gain, $\rho > 1$.

At an input orientation of 0° and 90° , the linear input is injected along the TE and TM mode respectively; these modes propagate and are amplified along their mode. This indicates that there is no modification on the principal axes over this power range. Within the range of injected power, the gain ratio ρ decreases to a value of 1.04 for an injected power of 2.2 mW indicating that the single-pass TE gain approximates to the single-pass TM gain.

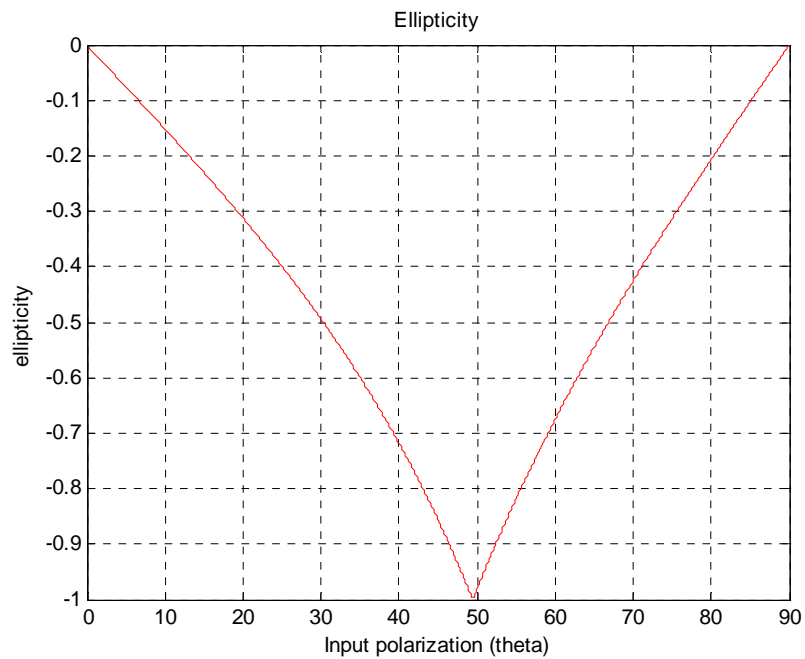


Figure 17: Output ellipticity as a function of Input Polarization angle. (Test4.m)

With the ellipticity graphic we can corroborate some previous deductions like $\rho > 1$. The fact that the minimum is reached at an angle greater than 45° reaffirms that the TE gain is greater than the TM gain.

The negative sign shows that the output polarisation is of left-handed rotation, indicating that the TE axis is slower than the TM axis. At 0° and 90° the ellipticity is zero, the linear input is injected along the TE and TM mode respectively, propagates and is amplified along its mode. This indicates that there is no modification on the principal axes over this power range.

3.4 Orthogonality

In this section the results for the scheme with two orthogonal signals are presented. In this case nonlinearities in the SOA affect to output orthogonality between the two signals, owing to each one of them undergoes a different nonlinear polarization rotation through the SOA. Input polarization rotation and input power are studied.

A. OUTPUT POLARIZATION ORIENTATION VS INPUT POLARIZATION ORIENTATION

We can see the effect of this rotation for different cases with high level signal power and low level signal power. In figures 17 y 18 we have depicted output polarization orientation as a function of input polarization orientation. This variation is more lineal for high level signal power.

The behaviour is similar to last section. At an input orientation of 0° and 90° , the linear input is injected along the TE and TM mode respectively and there is not polarization rotation.

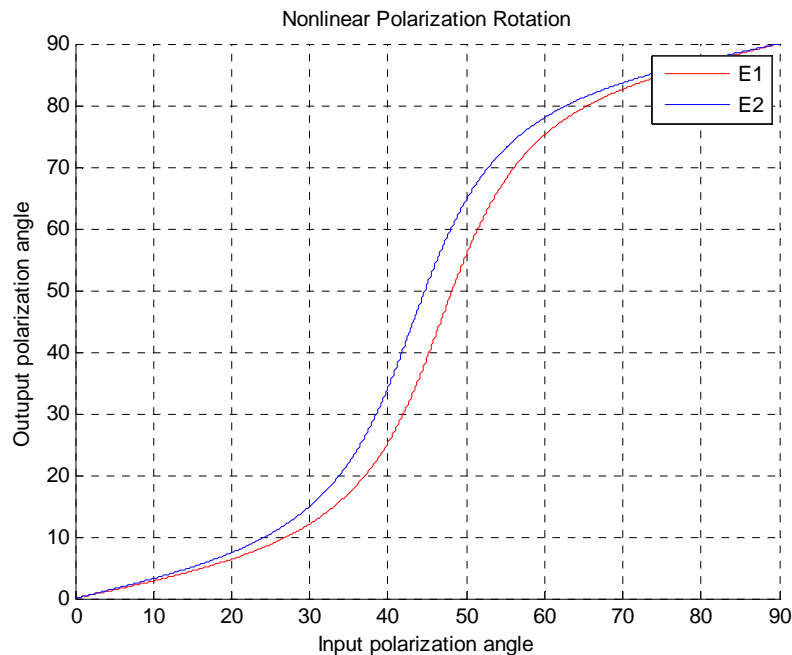


Figure 18: Output Polarization Angle as a function of Input polarization angle for E_1 and E_2 . Data signal='0' (Test5_zero.m)

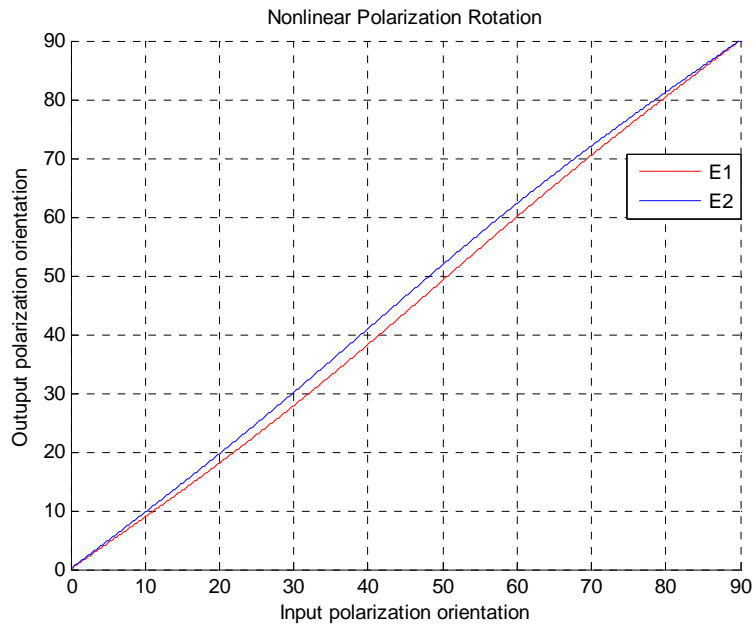


Figure 19: Output Polarization Angle as a function of Input polarization angle for E_1 and E_2 . Data signal='1' (Test5_one.m)

B. OUTPUT ORTHOGONALITY VS INPUT POLARIZATION ORIENTATION

In order to see how orthogonality is affected, we can base on last figures. We can depict the difference between E_1 and E_2 for both cases. 0° in y axis means two signals entirely orthogonal, whereas a certain angle means the deviation from perfect orthogonality.

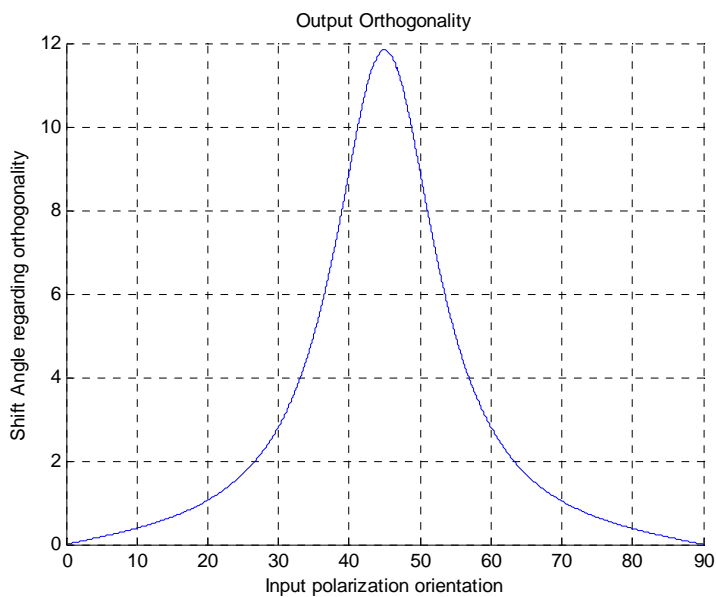


Figure 20: Shift Angle regarding orthogonality as a function of Input polarization angle for low level signal power. (Test5_zero.m)

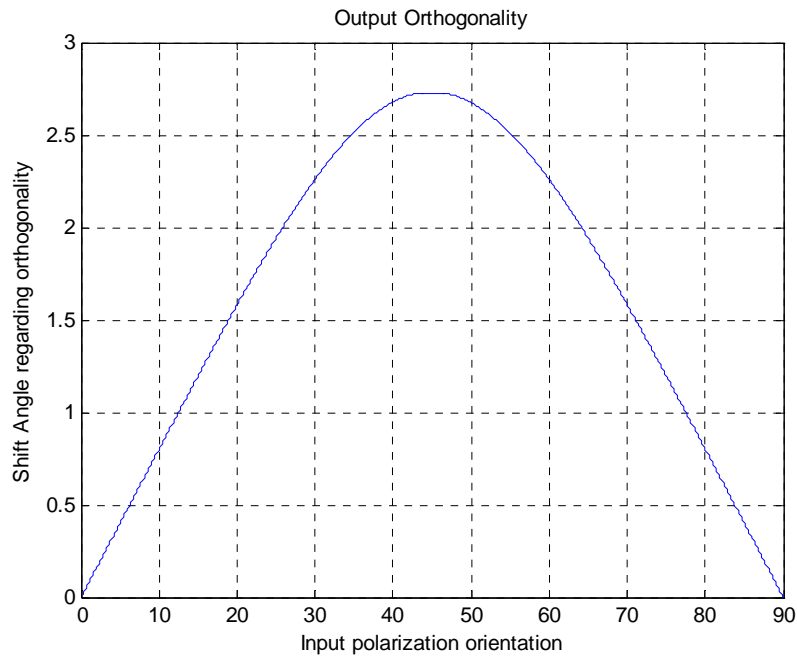


Figure 21: Shift Angle regarding orthogonality as a function of Input polarization angle for high level signal power. (Test5_one.m)

It is easy to see how the lost of orthogonality is greater for low level signal power. In the worst case we can have variation of up to 12° regarding to orthogonality. The best input polarization angle to preserve orthogonality in both cases is 45° . That is, the same energy injected along TE and TM modes.

C. OUTPUT ORTHOGONALITY VS INPUT PROBE SIGNAL POWER

We have gotten previous results carrying out the simulations with the optimal probe power found in the section 3.2. But it is very important too, to check this orthogonality using other values of probe power around the optimal value.

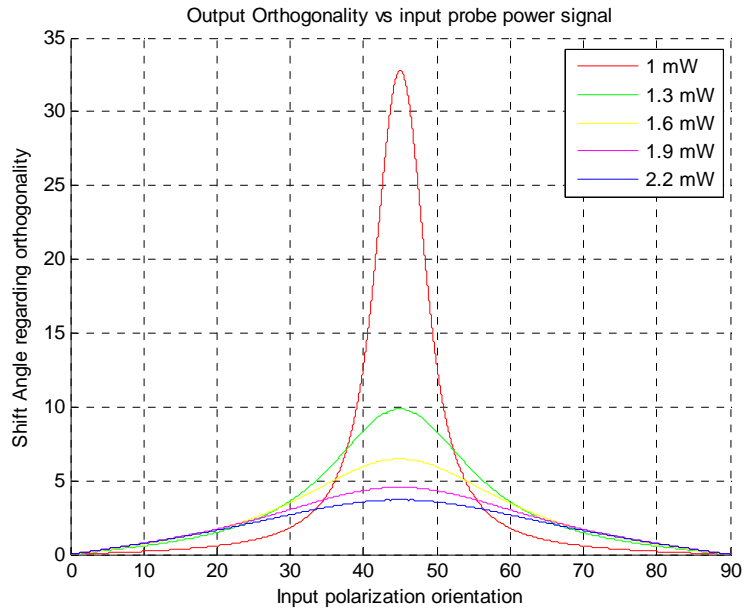


Figure 22: Orthogonality as a function of Input polarization angle for different levels of power. Data signal = 0. (Test6_zero.m)

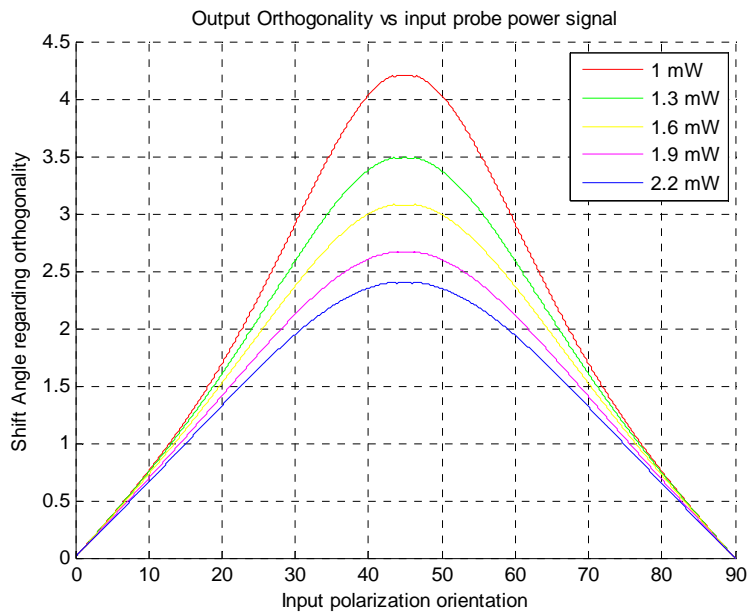


Figure 23: Orthogonality as a function of Input polarization angle for different levels of power. Data signal = 1. (Test6_one.m)

We can see how with inappropriate level of probe power, the deviation from orthogonality is very considerable. With the optimal value, calculated in the section 3.2 the orthogonality loss is in a middle point, what means a correct agreement between orthogonality loss and SOA-MZI operation.

D. OUTPUT ORTHOGONALITY VS INPUT DATA SIGNAL POWER

When input data signal changes from '0' to '1', the change in output orthogonality is very close to the previous case. A variation in probe signal or data signal causes a similar change in output orthogonality. This result, is important to emphasize, is valid if we do not have into account the dynamic of wavelength conversion in the SOA, which is our case.

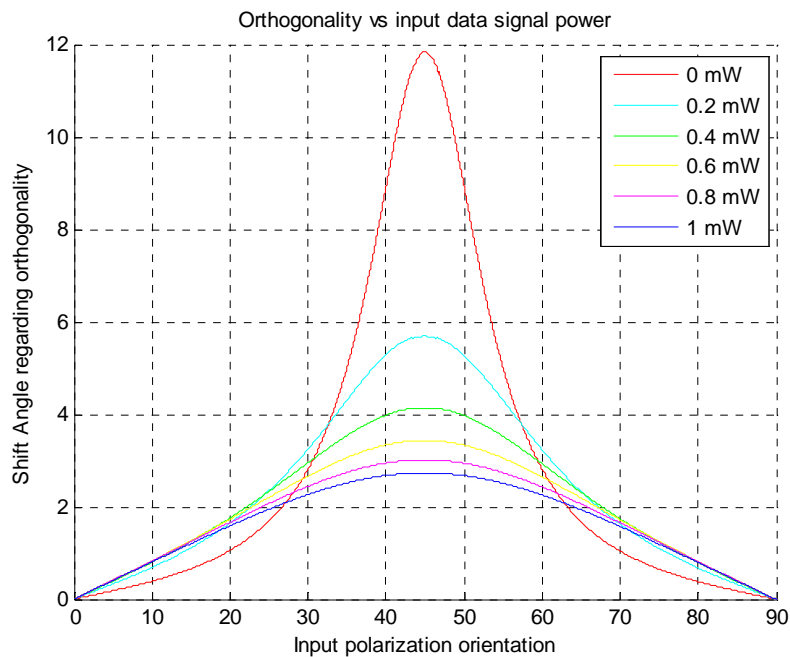


Figure 24: Orthogonality as a function of Input polarization angle for different levels of data signal power (test7.m)

E. OUTPUT ORTHOGONALTY VS INPUT PROBE SIGNAL POWER FOR CONSTANT INPUT ANGLE

In this section we have analyzed output orthogonality as a function of Input probe signal power for different input angles. This analysis has been done for optimal input probe signal and fixed value of input data signal.

As we can see in the figures, the behaviour of the SOA is totally different depending on input angle. It can present a decreasing response like the case for input polarization angle equal to 45° , or a different response, increasing for a certain levels of input power and decreasing for another, like the cases of input angles of 20° or 60° .

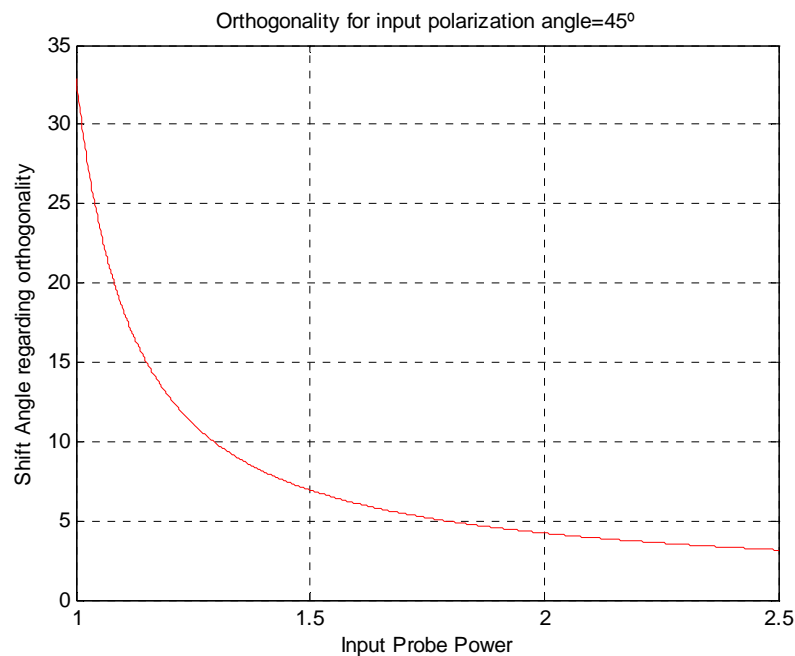


Figure 25: Orthogonality as a function of Input Probe Power for Input polarization angle = 45° . (TEST8.M)

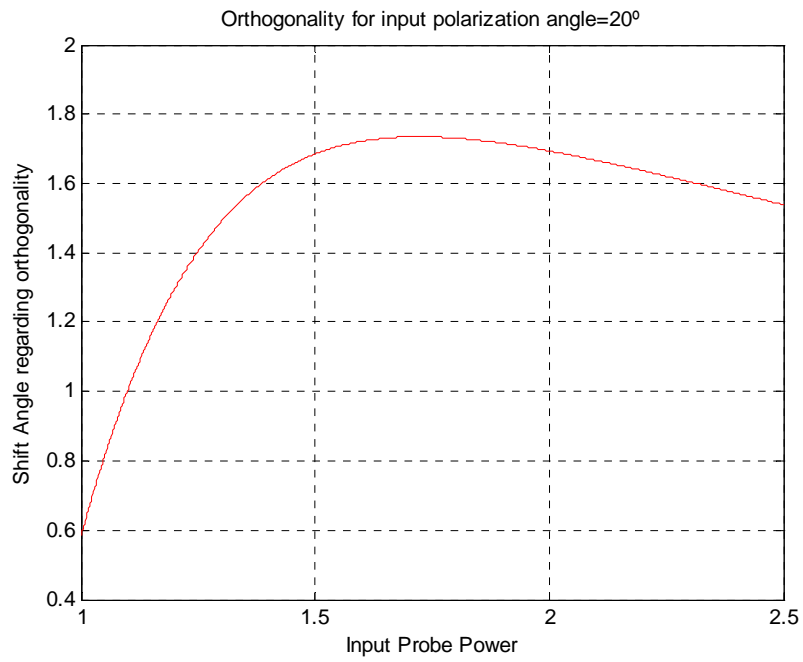


Figure 26: Orthogonality as a function of Input Probe Power for Input polarization angle = 20°

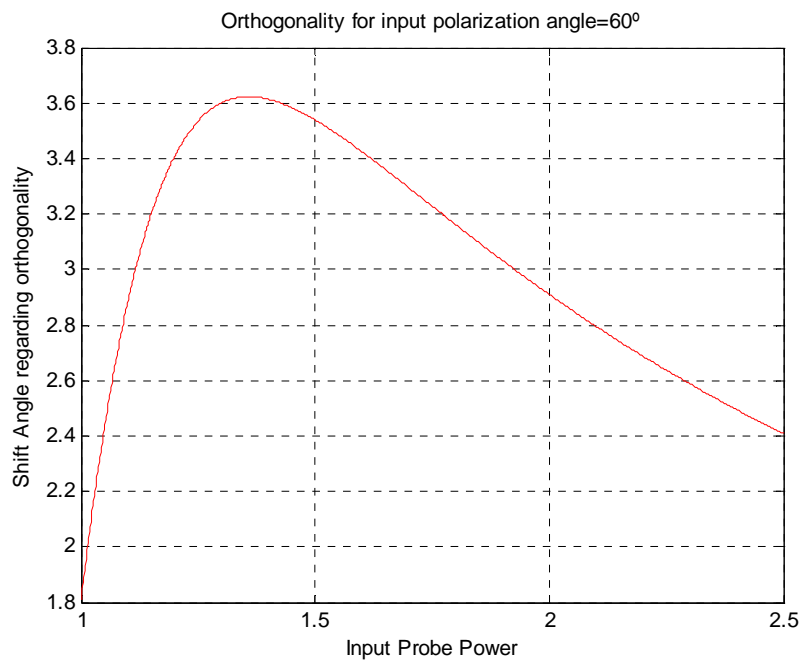


Figure 27: Orthogonality as a function of Input Probe Power for Input polarization angle = 60°

4. CONCLUSIONS

In the first part of this paper a detailed study of cross-phase wavelength conversion process in SOA's has been reported. We have seen how gain decrease with input power, and we have checked that the TE-TM gain ratio is greater than 1, therefore gain for TE mode is greater than gain for TM mode. We have calculated optimal value for input probe signal power for a correct operation of the SOA-MZI and we have seen that this power value is higher for TM mode than for TE mode owing to difference in guide refractive indexes and confinement factors.

A very important effect in our model is output ellipticity. It has been calculated as a function of input orientation. The ellipticity is measured for injected power of 1mW. As the injection angle increases, the ellipticity decreases, getting a minimum at 48°. At the minimum of ellipticity curves, the output is approaching a circular polarisation. The fact that the minimum is reached at an angle greater than 45° indicates that the TE gain must be greater than the TM gain. At 0° and 90° the ellipticity is zero; the linear input is injected along the TE and TM mode respectively, propagates and is amplified along this mode. This indicates that there is no modification of the principal axes over this power range. The simulation results are in good agreement with published experimental results [11].

The main model is based on the assumption that TE and TM components of the light have indirect interaction through the carriers. The TE and TM modes experience different refractive indexes, which lead to a phase difference between the two modes; this is the cause of nonlinear polarization rotation and loss of orthogonality between two signals. We have measured nonlinear polarisation changes in a SOA. The effect can clearly be significant, especially if the input polarisation angle is close to 45° to the TM and TE axes, and for low level signals power. We have measured the variation of the orthogonality with input polarization and input power, and we have seen, according to nonlinear polarization rotation, that this loss of orthogonality is greater for input polarization angles close to 45° and for low level signals power, being able to lose up to 33° regarding to orthogonality, for a signal of 1mW and input polarization angle of 45°. Excellent agreement has been found between our model and published experimental results.

These results are very important in order to get the best operation in the nodes of the OpMiGua network. With this study about polarization and output orthogonality we have a good base to start to work. We have an idea about power levels, input polarization angles, SOA's parameters..., with the aim of obtain the best demultiplexing results in the nodes. For future works, it would be a good idea to study in depth this model having into account time dynamics. Time dependency could be included in the model solving the differential equation number 1.

5. REFERENCES

- [1] "The OpMiGua Research Project". <http://www.opmigua.com>
- [2] Vegard L. Tuft, Jakob Buron, Dag R. Hjelme, and Steinar Bjørnstad. "Demonstration of an All-Optical Class-of-Service Segregation Method for Edge Nodes in Hybrid Circuit/Packet Switched Networks".
- [3] Terji Durhuus, Benny Mikkelsen, Carsten Joergensen, Soeren Lykke Danielsen, and Kristian E. Stubkjaer. "All-Optical Wavelength Conversion by Semiconductor Optical Amplifiers". JOURNAL OF LIGHTWAVE TECHNOLOGY, VOL. 14, NO. 6, JUNE 1996
- [4] Asghari, M., White, I.H., and Penty, R.V.: "Wavelength conversion using semiconductor optical amplifiers", J. Lightwave Technol., 1997, 15, (7), pp. 1181–1190
- [5] R.J. Manning, D.A.O. Davies and J.K. Lucek, "Recovery rates in Semiconductor Laser Amplifiers: Optical and Electrical Bias Dependencies", Elect. Lett. Vol 30, No 15, pp 1233-1234, 1994.
- [6] R.J. Manning, D.A.O. Davies. D. Cotter and J.K. Lucek. "Enhanced Recovery Rates in Semiconductor Laser Amplifiers using optical pumping", Elect. Lett. Vol30. No 10, pp 787-788, 1994.
- [7] Bipin Sankar Gopalakrishnapillai, Malin Premaratne, Ampalavanapillai Nirmalathas and Christina Lim. "Power Equalization Using Polarization Rotation in Semiconductor Optical Amplifiers" IEEE PHOTONICS TECHNOLOGY LETTERS, VOL. 17, NO. 8, AUGUST 2005
- [8] SOA Application Notes. <http://www.ciphotonics.com>
- [9] M. F. C. Stephens, M. Asghari, Member, IEEE, R. V. Penty, and I. H. White, "Demonstration of Ultrafast All-Optical Wavelength Conversion Utilizing Birefringence in Semiconductor Optical Amplifiers". IEEE PHOTONICS TECHNOLOGY LETTERS, VOL. 9, NO. 4, APRIL 1997
- [10] Vegard L. Tuft. "Polarization and Polarization Controllers". Version: October 9, 2006
- [11] B.F. Kennedy, S. Philippe, P. Landais, A.L. Bradley and H. Soto. "Experimental investigation of polarisation rotation in semiconductor optical amplifiers". IEE Proc.-Optoelectron., Vol. 151, No. 2, April 2004.

6. ACKNOWLEDGEMENTS

If I wanted to write about all the people that I am grateful to them, I should hurry up because otherwise I wouldn't have enough time in one life.

Therefore I only want to thank my supervisor Dag Roar Hjelme for welcoming and helping me whenever I have needed it. And moreover, to Vegard Larsen Tuft because without his help I doubt that I would have finished this thesis.

6. APPENDIX

In the appendix the most important Matlab functions developed are presented.

```
function I_optimal_TE=test2_TE
```

```
%
%-----
% Name:      test2_TE.m
% Author:    Raúl Martín
%-----
%
% Phase shift for TE mode as a function of Input probe signal power
% I_optimal_TE: optimal value for correct operation of the SOA-MZI
% NOTE: test2_TM.m is equal but using parameters for TM mode.
%
j=10e7;           % A/m^2   drive current density
q=1.6e-19;       % C       electronic charge
L=500e-6;        % m       SOA length
d=0.15e-6;       % m       active layer thickness
w=1.2e-6;        %
a1TE= 2.5e-20;   % m^2     material gain constant
a1TM=2.14e-20;   %
n0=1.1e24;       % m^-3    transparency carrier density
St=0;           %         average amplified spontaneous
                    emission
Ts=1e-9;        % s       carrier recombination life time

I_optical=0.5e-3:0.01e-3:2e-3; % W   Input optical power señal probe
I=I_optical./(d*w); % W/m^2   Input intensity
Iprobe=1.3e-3/(d*w);
Idatal=1e-3/(d*w);
Idata0=0;

h=6.6260693e-34;
v=1.935483e14;
E=h*v;

landa=1.55e-6;   % m
gammaTE=0.3;     %         Confinement factor TE
gammaTM=0.18;    %         Confinement factor TM
NrTE=3.1;        %         guide refractive index TE
NrTM=2.9;        %         guide refractive index TM
dN=-1.8e-26;    % m^3     Change in refractive index with
                    carrier density
```

```

% value of carrier concentration for zero input power
np_TE=(j/(q*d)+a1TE*n0*Iprobe/E+a1TE*n0*St)/(1/Ts+a1TE*Iprobe/E+a1TE*St);

for i=1:1:151;

% value of carrier density for data signal equal to one and zero
respectively

    n_one_TE(i)=(j/(q*d)+a1TE*n0*I(i)/E+a1TE*n0*Idatal/E+a1TE*n0*St)/
    (1/Ts+a1TE*I(i)/E+a1TE*Idatal/E+a1TE*St);

    n_zero_TE(i)=(j/(q*d)+a1TE*n0*I(i)/E+a1TE*n0*Idata0/E+a1TE*n0*St)/
    (1/Ts+a1TE*I(i)/E+a1TE*Idata0/E+a1TE*St);

% Nonlinear phase change fot data signal equal to one and zero

    phaseTE_one(i)=2*pi*L*(NrTE+gammaTE*np_TE*dN)/landa+2*pi*L*gammaTE*
    (n_one_TE(i)-np_TE)*dN/landa;

    phaseTE_zero(i)=2*pi*L*(NrTE+gammaTE*np_TE*dN)/landa+2*pi*L*gammaTE*
    (n_zero_TE(i)-np_TE)*dN/landa;

% Phase shift along SOA

    phaseTE_one_shift(i)=phaseTE_one(i)-phaseTE_one(1);

    phaseTE_zero_shift(i)=phaseTE_zero(i)-phaseTE_zero(1);

    difference(i)=phaseTE_one_shift(i)-phaseTE_zero_shift(i)+pi;
end

% To get the optimal value

min_difference=min(abs(difference));

for i=1:1:151
    if(abs(difference(i))==min_difference)
        I_optimal_TE=I_optical(i);
    end
end

plot(I_optical,phaseTE_zero_shift,'r', I_optical,phaseTE_one_shift,'b');
title('Phase shift for TE mode');
xlabel('Input probe power(W)')
ylabel('phase shift (rad)')
legend('data signal="0"', 'data signal="1"')
grid
end

% _____

```



```

function test3

%
%-----
%
% Name:      test3.m
%
% Author:    Raúl Martín
%
%-----
%
%
% Output polarization angle as a function of Input polarization
% angle for different levels of input power
%
%
j=10e7;           % A/m^2      drive current density
q=1.6e-19;       % C          electronic charge
d=0.15e-6;       % m          active layer thickness
a1TE= 2.5e-20;   % m^2        material gain constant
a1TM=2.14e-20;
n0=1.1e24;       % m^-3      transparency carrier density
St=0;           %          average amplified spontaneous
                    emission
Ts=1e-9;        % s          carrier recombination life time
w=1.2e-6;
Iprobe_inicial=0.5/(d*w);
St=0;
h=6.6260693e-34; % J*s
v=1.935483e14;  %
E=h*v;
L=500e-6;       % m          SOA length
landa=1.55e-6;  % m
gammaTE=0.3;    %          Confinement factor TE
gammaTM=0.24;   %          Confinement factor TM
NrTE=3.1;       %          guide refractive index TE
NrTM=2.9;       %          guide refractive index TM
dN=-1.2e-26;    % m^3        Change in refractive index with
                    carrier density

% different values for probe signal around optimal value

Iprobe=[1e-3, 1.3e-3, 1.55e-3, 1.9e-3, 2.2e-3]/(d*w);
Idata=0;

for i=1:1:5

% value of carrier concentration for zero input power

    np_TE(i)=(j/(q*d)+a1TE*n0*Iprobe(i)/E+a1TE*n0*St)/(1/Ts+a1TE*
    Iprobe(i)/E+a1TE*St)

    np_TM(i)=(j/(q*d)+a1TM*n0*Iprobe(i)/E+a1TM*n0*St)/(1/Ts+a1TM*
    Iprobe(i)/E+a1TM*St)

% initial value of carrier density to calculate only the relative value
% later, not the absolute value.

n_inicial_TE=(j/(q*d)+a1TE*n0*Iprobe_inicial/E+a1TE*n0*Idata/E+a1TE*
n0*St)/(1/Ts+a1TE*Iprobe_inicial/E+a1TE*Idata/E+a1TE*St);

```

Polarization Effects in Wavelength Converters based on Semiconductor Optical Amplifiers

```

n_inicial_TM=(j/(q*d)+a1TM*n0*Iprobe_inicial/E+a1TM*n0*Idata/E+a1TM*
n0*St)/(1/Ts+a1TM*Iprobe_inicial/E+a1TM*Idata/E+a1TM*St);

% value of carrier density

n_TE(i)=(j/(q*d)+a1TE*n0*Idata/E+a1TE*n0*Iprobe(i)/E+a1TE*n0*St)/(1/
Ts+a1TE*Idata/E+a1TE*Iprobe(i)/E+a1TE*St);

n_TM(i)=(j/(q*d)+a1TM*n0*Idata/E+a1TM*n0*Iprobe(i)/E+a1TM*n0*St)/(1/
Ts+a1TM*Idata/E+a1TM*Iprobe(i)/E+a1TM*St);

% value of initial phase

phaseTE_inicial(i)=2*pi*L*(NrTE+gammaTE*np_TE(i)*dN)/landa+2*pi*L*
gammaTE*(n_inicial_TE-np_TE(i))*dN/landa;

phaseTM_inicial(i)=2*pi*L*(NrTM+gammaTM*np_TM(i)*dN)/landa+2*pi*L*
gammaTM*(n_inicial_TM-np_TM(i))*dN/landa;

% Nonlinear phase change

phaseTE(i)=2*pi*L*(NrTE+gammaTE*np_TE(i)*dN)/landa+2*pi*L*gammaTE*
(n_TE(i)-np_TE(i))*dN/landa;

phaseTM(i)=2*pi*L*(NrTM+gammaTM*np_TM(i)*dN)/landa+2*pi*L*gammaTM*
(n_TM(i)-np_TM(i))*dN/landa;

% Phase shift along SOA

phaseTE_shift(i)=phaseTE(i)-phaseTE_inicial(i)
phaseTM_shift(i)=phaseTM(i)-phaseTM_inicial(i);

% Phase difference between TM and TE modes

delta_fi_out(i)=phaseTM_shift(i)-phaseTE_shift(i);

% Gain for TE and TM modes. Gain ratio

gain_TE(i)=a1TE*(n_TE(i)-n0);
gain_TM(i)=a1TM*(n_TM(i)-n0);
gain_ratio(i)=gain_TE(i)/gain_TM(i);

end

% Input polarization angle
theta=0:pi/2/10000:pi/2;

% These lines are to avoiding working with matrix.

gain_ratio_02=gain_ratio(1);
gain_ratio_04=gain_ratio(2);
gain_ratio_06=gain_ratio(3);
gain_ratio_08=gain_ratio(4);
gain_ratio_10=gain_ratio(5);

Iprobe02=Iprobe(1);
Iprobe04=Iprobe(2);
Iprobe06=Iprobe(3);
Iprobe08=Iprobe(4);
Iprobe10=Iprobe(5);

```

Polarization Effects in Wavelength Converters based on Semiconductor Optical Amplifiers

```

delta_fi_out_02=delta_fi_out(1);
delta_fi_out_04=delta_fi_out(2);
delta_fi_out_06=delta_fi_out(3);
delta_fi_out_08=delta_fi_out(4);
delta_fi_out_10=delta_fi_out(5);

for i=1:1:10001

% Eo_TE and Eo_TM as a function of input polarization angle and Iprobe

    Eo_TE_1_02(i)=(gain_ratio_02.*sqrt(Iprobe02).*cos(theta(i)));
    Eo_TE_1_04(i)=(gain_ratio_04.*sqrt(Iprobe04).*cos(theta(i)));
    Eo_TE_1_06(i)=(gain_ratio_06.*sqrt(Iprobe06).*cos(theta(i)));
    Eo_TE_1_08(i)=(gain_ratio_08.*sqrt(Iprobe08).*cos(theta(i)));
    Eo_TE_1_10(i)=(gain_ratio_10.*sqrt(Iprobe10).*cos(theta(i)));

    Eo_TM_1_02(i)=sqrt(Iprobe02).*sin(theta(i));
    Eo_TM_1_04(i)=sqrt(Iprobe04).*sin(theta(i));
    Eo_TM_1_06(i)=sqrt(Iprobe06).*sin(theta(i));
    Eo_TM_1_08(i)=sqrt(Iprobe08).*sin(theta(i));
    Eo_TM_1_10(i)=sqrt(Iprobe10).*sin(theta(i));

% Previous output polarization angle

    psi_previol_02(i)=1/2*atan(2.*Eo_TM_1_02(i).*Eo_TE_1_02(i)*
    cos(delta_fi_out_02)/(Eo_TE_1_02(i).^2-Eo_TM_1_02(i).^2));
    psi_previol_04(i)=1/2*atan(2.*Eo_TM_1_04(i).*Eo_TE_1_04(i)*
    cos(delta_fi_out_04)/(Eo_TE_1_04(i).^2-Eo_TM_1_04(i).^2));
    psi_previol_06(i)=1/2*atan(2.*Eo_TM_1_06(i).*Eo_TE_1_06(i)*
    cos(delta_fi_out_06)/(Eo_TE_1_06(i).^2-Eo_TM_1_06(i).^2));
    psi_previol_08(i)=1/2*atan(2.*Eo_TM_1_08(i).*Eo_TE_1_08(i)*
    cos(delta_fi_out_08)/(Eo_TE_1_08(i).^2-Eo_TM_1_08(i).^2));
    psi_previol_10(i)=1/2*atan(2.*Eo_TM_1_10(i).*Eo_TE_1_10(i)*
    cos(delta_fi_out_10)/(Eo_TE_1_10(i).^2-Eo_TM_1_10(i).^2));

end

% All these lines of code, are for avoiding a discontinuity of the
function tangent in the equation to calculate output polarization angle

difference_1_02=max(psi_previol_02)-min(psi_previol_02);
difference_1_04=max(psi_previol_04)-min(psi_previol_04);
difference_1_06=max(psi_previol_06)-min(psi_previol_06) ;
difference_1_08=max(psi_previol_08)-min(psi_previol_08);
difference_1_10=max(psi_previol_10)-min(psi_previol_10);

for i=1:1:10000
    if(abs(psi_previol_02(i+1)-psi_previol_02(i))>0.5)
        frontera_tectal_02=theta(i+1);
    end
end

for i=1:1:10001
    if(theta(i)>=(frontera_tectal_02))
        psi_1_02(i)=psi_previol_02(i)+difference_1_02;
    else
        psi_1_02(i)=psi_previol_02(i);
    end
end
end

```

```

for i=1:1:10000
    if(abs(psi_previol_04(i+1)-psi_previol_04(i))>0.5)
        frontera_tectal_04=theta(i+1);
    end
end

for i=1:1:10001
    if(theta(i)>=(frontera_tectal_04))
        psi_1_04(i)=psi_previol_04(i)+difference_1_04;
    else
        psi_1_04(i)=psi_previol_04(i);
    end
end

for i=1:1:10000
    if(abs(psi_previol_06(i+1)-psi_previol_06(i))>0.5)
        frontera_tectal_06=theta(i+1);
    end
end

for i=1:1:10001
    if(theta(i)>=(frontera_tectal_06))
        psi_1_06(i)=psi_previol_06(i)+difference_1_06;
    else
        psi_1_06(i)=psi_previol_06(i);
    end
end

for i=1:1:10000
    if(abs(psi_previol_08(i+1)-psi_previol_08(i))>0.5)
        frontera_tectal_08=theta(i+1);
    end
end

for i=1:1:10001
    if(theta(i)>=(frontera_tectal_08))
        psi_1_08(i)=psi_previol_08(i)+difference_1_08;
    else
        psi_1_08(i)=psi_previol_08(i);
    end
end

for i=1:1:10000
    if(abs(psi_previol_10(i+1)-psi_previol_10(i))>0.5)
        frontera_tectal_10=theta(i+1);
    end
end

for i=1:1:10001
    if(theta(i)>=(frontera_tectal_10))
        psi_1_10(i)=psi_previol_10(i)+difference_1_10;
    else
        psi_1_10(i)=psi_previol_10(i);
    end
end

```

```
theta_degree=theta*180/pi;

psi_degree1_02=psi_1_02*180/pi;
psi_degree1_04=psi_1_04*180/pi;
psi_degree1_06=psi_1_06*180/pi;
psi_degree1_08=psi_1_08*180/pi;
psi_degree1_10=psi_1_10*180/pi;

hold
plot(theta_degree,psi_degree1_02, 'r');
plot(theta_degree,psi_degree1_04, 'g');
plot(theta_degree,psi_degree1_06, 'y');
plot(theta_degree,psi_degree1_08, 'm');
plot(theta_degree,psi_degree1_10, 'b');
xlabel('Input polarization orientation');
ylabel('Outuput polarization orientation');
title('Nonlinear Polarization Rotation');
legend('1 mW', '1.3 mW', '1.6 mW', '1.9 mW', '2.2 mW');
grid
end

%
```

```

function test4

%
%
% Name:      test4.m
%
% Author:    Raúl Martín
%
%
%
%
% Output ellipticity as a function of input polarization angle
% ellipticity = 0 means polarization is linear
% ellipticity = -1 means polarization is circular

j=10e7;           % A/m^2      drive current density
q=1.6e-19;        % C          electronic charge
d=0.15e-6;        % m          active layer thickness
a1TE= 2.5e-20;    % m^2       material gain constant
a1TM=2.14e-20;
n0=1.1e24;        % m^-3      transparency carrier density
St=0;            %          average amplified spontaneous
                    emission
Ts=1e-9;         % s          carrier recombination life time
w=1.2e-6;
Iprobe_inicial=0.5/(d*w);
St=0;
h=6.6260693e-34; % J*s
v=1.935483e14;   %
E=h*v;
Iprobe=1e-3/(d*w);
Idata=0;
L=500e-6;        % m          SOA length
landa=1.55e-6;   % m
gammaTE=0.3;     %          Confinement factor TE
gammaTM=0.24;    %          Confinement factor TM
NrTE=3.1;        %          guide refractive index TE
NrTM=2.9;        %          guide refractive index TM
dN=-1.2e-26;    % m^3       Change in refractive index with
                    carrier density

% value of carrier concentration for zero input power

np_TE= (j/(q*d)+a1TE*n0*Iprobe/E+a1TE*n0*St)/(1/Ts+a1TE*Iprobe/E+a1TE*St);
np_TM= (j/(q*d)+a1TM*n0*Iprobe/E+a1TM*n0*St)/(1/Ts+a1TM*Iprobe/E+a1TM*St);

% initial value of carrier density to calculate only the relative value
later, not the absolute value

n_inicial_TE=(j/(q*d)+a1TE*n0*Iprobe_inicial/E+a1TE*n0*Idata/E+a1TE*n0*St)/
/(1/Ts+a1TE*Iprobe_inicial/E+a1TE*Idata/E+a1TE*St);

n_inicial_TM=(j/(q*d)+a1TM*n0*Iprobe_inicial/E+a1TM*n0*Idata/E+a1TM*n0*St)/
/(1/Ts+a1TM*Iprobe_inicial/E+a1TM*Idata/E+a1TM*St);

% value of carrier density

n_TE=(j/(q*d)+a1TE*n0*Idata/E+a1TE*n0*Iprobe/E+a1TE*n0*St)/
(1/Ts+a1TE*Idata/E+a1TE*Iprobe/E+a1TE*St);

```

```

n_TM=(j/(q*d)+a1TM*n0*Idata/E+a1TM*n0*Iprobe/E+a1TM*n0*St)/
(1/Ts+a1TM*Idata/E+a1TM*Iprobe/E+a1TM*St);

% initial phase

phaseTE_inicial=2*pi*L*(NrTE+gammaTE*np_TE*dN)/landa+2*pi*L*gammaTE*
(n_inicial_TE-np_TE)*dN/landa;

phaseTM_inicial=2*pi*L*(NrTM+gammaTM*np_TM*dN)/landa+2*pi*L*gammaTM*
(n_inicial_TM-np_TM)*dN/landa;

% Nonlinear phase change

phaseTE=2*pi*L*(NrTE+gammaTE*np_TE*dN)/landa+2*pi*L*gammaTE*(n_TE-np_TE)
*dN/landa;

phaseTM=2*pi*L*(NrTM+gammaTM*np_TM*dN)/landa+2*pi*L*gammaTM*(n_TM-np_TM)
*dN/landa;

% Phase shift along SOA
phaseTE_shift=phaseTE-phaseTE_inicial;
phaseTM_shift=phaseTM-phaseTM_inicial;

% Phase difference between TM and TE modes
delta_fi_out=phaseTM_shift-phaseTE_shift;
theta=0:pi/2/10000:pi/2;

% Gain for TE and TM modes. Gain ratio
gain_TE=a1TE*(n_TE-n0);
gain_TM=a1TM*(n_TM-n0);
gain_ratio=gain_TE/gain_TM;

for i=1:1:10001

    % Eo_TE and Eo_TM as a function of input polarization angle
    E0_TE_1(i)=(gain_ratio.*sqrt(Iprobe).*cos(theta(i)));
    E0_TM_1(i)=sqrt(Iprobe).*sin(theta(i));

    % Previous output polarization angle

    psi_previo1(i)=1/2*atan(2.*E0_TM_1(i).*E0_TE_1(i)*cos(delta_fi_out)/
(E0_TE_1(i).^2-E0_TM_1(i).^2));
end

for i=1:1:10001
    if (E0_TM_1(i)<E0_TE_1(i)*gain_ratio)
        elip(i)=E0_TM_1(i)./(E0_TE_1(i).*gain_ratio);
    else
        elip(i)=E0_TE_1(i).*gain_ratio./E0_TM_1(i);
    end
end

theta_degree=theta*180/pi;
plot(theta_degree, -elip, 'r');
xlabel('Input polarization (theta)');
ylabel('ellipticity');
title('Ellipticity')
grid
end
%
```

```

function test5_zero

%
%
% Name:      test5_zero.m
%
% Author:    Raúl Martín
%
%
%
%
% Output polarization angle as a function of input polarization
% angle for E1 and E2, and data signal='0'
%
% Output Orthogonality as a function of Input polarization angle
% for data signal = '0'
%
% NOTE: test5_one.m is equal but using Idata1

j=10e7;           % A/m^2      drive current density
q=1.6e-19;        % C          electronic charge
d=0.15e-6;        % m          active layer thickness
a1TE= 2.5e-20;    % m^2        material gain constant
a1TM=2.14e-20;
n0=1.1e24;        % m^-3       transparency carrier density
St=0;            %           average amplified spontaneous
                    emission
Ts=1e-9;         % s          carrier recombination life
                    time

w=1.2e-6;
Iprobe=1.55e-3/(d*w);
Iprobe_inicial=0.5e-3/(d*w);
St=0;
h=6.6260693e-34; % J*s
v=1.935483e14;   %
E=h*v;
Idata1=1e-3/(d*w);
Idata0=0;
L=500e-6;        % m          SOA length
landa=1.55e-6;   % m
gammaTE=0.3;     %           Confinement factor TE
gammaTM=0.24;    %           Confinement factor TM
NrTE=3.1;        %           guide refractive index TE
NrTM=2.9;        %           guide refractive index TM
dN=-1.2e-26;    %           m^3 Change in refractive index
with            carrier density

% value of carrier concentration for zero input power

np_TE= (j/(q*d)+a1TE*n0*Iprobe/E+a1TE*n0*St)/(1/Ts+a1TE*Iprobe/E+a1TE*St);
np_TM= (j/(q*d)+a1TM*n0*Iprobe/E+a1TM*n0*St)/(1/Ts+a1TM*Iprobe/E+a1TM*St);

% initial value of carrier density to calculate only the relative value
later, not the absolute value

n_zero_inicial_TE=(j/(q*d)+a1TE*n0*Iprobe_inicial/E+a1TE*n0*Idata0/E+
a1TE*n0*St)/(1/Ts+a1TE*Iprobe_inicial/E+a1TE*Idata0/E+a1TE*St);

```



```

n_zero_inicial_TM=(j/(q*d)+a1TM*n0*Iprobe_inicial/E+a1TM*n0*Idata0/E+
a1TM*n0*St)/(1/Ts+a1TM*Iprobe_inicial/E+a1TM*Idata0/E+a1TM*St);

% value of carrier density

n_zero_TE=(j/(q*d)+a1TE*n0*Iprobe/E+a1TE*n0*Idata0/E+a1TE*n0*St)/
(1/Ts+a1TE*Iprobe/E+a1TE*Idata0/E+a1TE*St);

n_zero_TM=(j/(q*d)+a1TM*n0*Iprobe/E+a1TM*n0*Idata0/E+a1TM*n0*St)/
(1/Ts+a1TM*Iprobe/E+a1TM*Idata0/E+a1TM*St);

% initial phase

phaseTE_zero_inicial=2*pi*L*(NrTE+gammaTE*np_TE*dN)/landa+2*pi*L*
gammaTE*(n_zero_inicial_TE-np_TE)*dN/landa;

phaseTM_zero_inicial=2*pi*L*(NrTM+gammaTM*np_TM*dN)/landa+2*pi*L*
gammaTM*(n_zero_inicial_TM-np_TM)*dN/landa;

% Nonlinear phase change

phaseTE_zero=2*pi*L*(NrTE+gammaTE*np_TE*dN)/landa+2*pi*L*gammaTE*
(n_zero_TE-np_TE)*dN/landa;

phaseTM_zero=2*pi*L*(NrTM+gammaTM*np_TM*dN)/landa+2*pi*L*gammaTM*
(n_zero_TM-np_TM)*dN/landa;

% Phase shift along SOA

phaseTE_zero_shift=phaseTE_zero-phaseTE_zero_inicial;
phaseTM_zero_shift=phaseTM_zero-phaseTM_zero_inicial;

% Phase difference between TM and TE modes
delta_fi_out_zero=phaseTM_zero_shift-phaseTE_zero_shift;

% Gain for TE and TM modes. Gain ratio

gain_zero_TE=a1TE*(n_zero_TE-n0);
gain_zero_TM=a1TM*(n_zero_TM-n0);
gain_ratio_zero=gain_zero_TE/gain_zero_TM;

theta=0:pi/2/10000:pi/2;

for i=1:1:10001

    % Eo_TE and Eo_TM as a function of input polarization angle
    Eo_TE_zero1(i)=(gain_ratio_zero.*sqrt(Iprobe).*cos(theta(i)));
    Eo_TE_zero2(i)=-gain_ratio_zero.*sqrt(Iprobe).*cos(pi/2-theta(i));

    Eo_TM1(i)=sqrt(Iprobe).*sin(theta(i));
    Eo_TM2(i)=sqrt(Iprobe).*sin(pi/2-theta(i));

    % Previous output polarization angle
    psi_zero_previo1(i)=1/2*atan(2.*Eo_TM1(i).*Eo_TE_zero1(i)*
cos(delta_fi_out_zero)/(Eo_TE_zero1(i).^2-Eo_TM1(i).^2));

    psi_zero_previo2(i)=1/2*atan(2.*Eo_TM2(i).*Eo_TE_zero2(i)*
cos(delta_fi_out_zero)/(Eo_TE_zero2(i).^2-Eo_TM2(i).^2));

end

```

```

% All these lines of code, are for avoiding a discontinuity of the
% function tangent in the equation to calculate output polarization
% angle

difference_zero1=max(psi_zero_previo1)-min(psi_zero_previo1);
difference_zero2=max(psi_zero_previo2)-min(psi_zero_previo2);

for i=1:1:10000
    if(abs(psi_zero_previo1(i+1)-psi_zero_previo1(i))>0.5)
        frontera_theta_zero1=theta(i+1);
    end
end

for i=1:1:10001
    if(theta(i)>=(frontera_theta_zero1))
        psi_zero1(i)=psi_zero_previo1(i)+difference_zero1;
    else
        psi_zero1(i)=psi_zero_previo1(i);
    end
end

for i=1:1:10000
    if(abs(psi_zero_previo2(i+1)-psi_zero_previo2(i))>0.5)
        frontera_theta_zero2=theta(i+1);
    end
end

for i=1:1:10001
    if(theta(i)>=(frontera_theta_zero2))
        psi_zero2(i)=psi_zero_previo2(i)+difference_zero2;
    else
        psi_zero2(i)=psi_zero_previo2(i);
    end
end

dif_orthogonality=psi_zero2-psi_zero1;
dif_orthogonality_degree=dif_orthogonality*180/pi;

psi_zero_degree1=psi_zero1*180/pi;
psi_zero_degree2=psi_zero2*180/pi;
theta_degree=theta*180/pi;

subplot(2,1,1)
hold
plot(theta_degree,psi_zero_degree1, 'r');
plot(theta_degree,psi_zero_degree2, 'b');
xlabel('Input polarization angle');
ylabel('Outuput polarization angle');
title('Nonlinear Polarization Rotation');
legend('E1', 'E2');
grid
subplot(2,1,2)
plot(theta_degree,dif_orthogonality_degree);
title('Output Orthogonality')
xlabel('Input polarization orientation');
ylabel('Shift Angle regarding orthogonality');
grid
end
%

```

```

function test6_zero

%
%
% Name:      test6_zero.m
%
% Author:    Raúl Martín
%
%
%
% Orthogonality as a function of Input polarization angle for
% different
% levels of power. Data signal = '0'.
%
% NOTE: test6_one.m is equal but with data signal='1'

j=10e7;           % A/m^2      drive current density
q=1.6e-19;        % C          electronic charge
d=0.15e-6;        % m          active layer thickness
a1TE= 2.5e-20;    % m^2        Material gain constant
a1TM=2.14e-20;
n0=1.1e24;        % m^-3       transparency carrier density
St=0;             %           average amplified spontaneous
                    emission
Ts=1e-9;          % s          carrier recombination life
                    time

w=1.2e-6;
Iprobe_inicial=0.5/(d*w);
St=0;
h=6.6260693e-34; % J*s
v=1.935483e14;   %
E=h*v;
Idata=0;
L=500e-6;        % m          SOA length
landa=1.55e-6;   % m
gammaTE=0.3;     %           Confinement factor TE
gammaTM=0.24;    %           Confinement factor TM
NrTE=3.1;        %           guide refractive index TE
NrTM=2.9;        %           guide refractive index TM
dN=-1.2e-26;    % m^3        Change in refractive index with
                    carrier density

Iprobe=[1e-3, 1.3e-3, 1.55e-3, 1.9e-3, 2.2e-3]/(d*w);

for i=1:1:5

    % value of carrier concentration for zero input power

    np_TE(i)=(j/(q*d)+a1TE*n0*Iprobe(i)/E+a1TE*n0*St)/(1/Ts+a1TE*
    Iprobe(i)/E+a1TE*St);

    np_TM(i)=(j/(q*d)+a1TM*n0*Iprobe(i)/E+a1TM*n0*St)/(1/Ts+a1TM*
    Iprobe(i)/E+a1TM*St);

```

```

% initial value of carrier density to calculate only the
% relative value later, not the absolute value

n_inicial_TE=(j/(q*d)+a1TE*n0*Iprobe_inicial/E+a1TE*n0*Idata/E+
a1TE*n0*St)/(1/Ts+a1TE*Iprobe_inicial/E+a1TE*Idata/E+a1TE*St);

n_inicial_TM=(j/(q*d)+a1TM*n0*Iprobe_inicial/E+a1TM*n0*Idata/E+
a1TM*n0*St)/(1/Ts+a1TM*Iprobe_inicial/E+a1TM*Idata/E+a1TM*St);

% value of carrier density

n_TE(i)=(j/(q*d)+a1TE*n0*Idata/E+a1TE*n0*Iprobe(i)/E+a1TE*n0*St)
/(1/Ts+a1TE*Idata/E+a1TE*Iprobe(i)/E+a1TE*St);

n_TM(i)=(j/(q*d)+a1TM*n0*Idata/E+a1TM*n0*Iprobe(i)/E+a1TM*n0*St)
/(1/Ts+a1TM*Idata/E+a1TM*Iprobe(i)/E+a1TM*St);

% initial phase

phaseTE_inicial(i)=2*pi*L*(NrTE+gammaTE*np_TE(i)*dN)/landa+2*pi*L*
gammaTE*(n_inicial_TE-np_TE(i))*dN/landa;

phaseTM_inicial(i)=2*pi*L*(NrTM+gammaTM*np_TM(i)*dN)/landa+2*pi*L*
gammaTM*(n_inicial_TM-np_TM(i))*dN/landa;

% Nonlinear phase change

phaseTE(i)=2*pi*L*(NrTE+gammaTE*np_TE(i)*dN)/landa+2*pi*L*gammaTE*
(n_TE(i)-np_TE(i))*dN/landa;

phaseTM(i)=2*pi*L*(NrTM+gammaTM*np_TM(i)*dN)/landa+2*pi*L*gammaTM*
(n_TM(i)-np_TM(i))*dN/landa;

% Phase shift along SOA

phaseTE_shift(i)=phaseTE(i)-phaseTE_inicial(i);
phaseTM_shift(i)=phaseTM(i)-phaseTM_inicial(i);

% Phase difference between TM and TE modes

delta_fi_out(i)=phaseTM_shift(i)-phaseTE_shift(i);

% Gain for TE and TM modes. Gain ratio
gain_TE(i)=a1TE*(n_TE(i)-n0);
gain_TM(i)=a1TM*(n_TM(i)-n0);
gain_ratio(i)=gain_TE(i)/gain_TM(i);
end

% Input polarization angle

theta=0:pi/2/10000:pi/2;

% These lines are to avoiding working with matrix.

gain_ratio_02=gain_ratio(1);
gain_ratio_04=gain_ratio(2);
gain_ratio_06=gain_ratio(3);
gain_ratio_08=gain_ratio(4);
gain_ratio_10=gain_ratio(5);

```

```

Iprobe02=Iprobe(1);
Iprobe04=Iprobe(2);
Iprobe06=Iprobe(3);
Iprobe08=Iprobe(4);
Iprobe10=Iprobe(5);

delta_fi_out_02=delta_fi_out(1);
delta_fi_out_04=delta_fi_out(2);
delta_fi_out_06=delta_fi_out(3);
delta_fi_out_08=delta_fi_out(4);
delta_fi_out_10=delta_fi_out(5);

for i=1:1:10001

    % Eo_TE and Eo_TM as a function of input polarization angle

    Eo_TE_1_02(i)=(gain_ratio_02.*sqrt(Iprobe02).*cos(theta(i)));
    Eo_TE_1_04(i)=(gain_ratio_04.*sqrt(Iprobe04).*cos(theta(i)));
    Eo_TE_1_06(i)=(gain_ratio_06.*sqrt(Iprobe06).*cos(theta(i)));
    Eo_TE_1_08(i)=(gain_ratio_08.*sqrt(Iprobe08).*cos(theta(i)));
    Eo_TE_1_10(i)=(gain_ratio_10.*sqrt(Iprobe10).*cos(theta(i)));

    Eo_TM_1_02(i)=sqrt(Iprobe02).*sin(theta(i));
    Eo_TM_1_04(i)=sqrt(Iprobe04).*sin(theta(i));
    Eo_TM_1_06(i)=sqrt(Iprobe06).*sin(theta(i));
    Eo_TM_1_08(i)=sqrt(Iprobe08).*sin(theta(i));
    Eo_TM_1_10(i)=sqrt(Iprobe10).*sin(theta(i));

    Eo_TE_2_02(i)=-gain_ratio_02.*sqrt(Iprobe02).*cos(pi/2-theta(i));
    Eo_TE_2_04(i)=-gain_ratio_04.*sqrt(Iprobe04).*cos(pi/2-theta(i));
    Eo_TE_2_06(i)=-gain_ratio_06.*sqrt(Iprobe06).*cos(pi/2-theta(i));
    Eo_TE_2_08(i)=-gain_ratio_08.*sqrt(Iprobe08).*cos(pi/2-theta(i));
    Eo_TE_2_10(i)=-gain_ratio_10.*sqrt(Iprobe10).*cos(pi/2-theta(i));

    Eo_TM_2_02(i)=sqrt(Iprobe02).*sin(pi/2-theta(i));
    Eo_TM_2_04(i)=sqrt(Iprobe04).*sin(pi/2-theta(i));
    Eo_TM_2_06(i)=sqrt(Iprobe06).*sin(pi/2-theta(i));
    Eo_TM_2_08(i)=sqrt(Iprobe08).*sin(pi/2-theta(i));
    Eo_TM_2_10(i)=sqrt(Iprobe10).*sin(pi/2-theta(i));

    % Previous output polarization angle

    psi_previol_02(i)=1/2*atan(2.*Eo_TM_1_02(i).*Eo_TE_1_02(i)*
    cos(delta_fi_out_02)/(Eo_TE_1_02(i).^2-Eo_TM_1_02(i).^2));

    psi_previol_04(i)=1/2*atan(2.*Eo_TM_1_04(i).*Eo_TE_1_04(i)*
    cos(delta_fi_out_04)/(Eo_TE_1_04(i).^2-Eo_TM_1_04(i).^2));

    psi_previol_06(i)=1/2*atan(2.*Eo_TM_1_06(i).*Eo_TE_1_06(i)*
    cos(delta_fi_out_06)/(Eo_TE_1_06(i).^2-Eo_TM_1_06(i).^2));

    psi_previol_08(i)=1/2*atan(2.*Eo_TM_1_08(i).*Eo_TE_1_08(i)*
    cos(delta_fi_out_08)/(Eo_TE_1_08(i).^2-Eo_TM_1_08(i).^2));

    psi_previol_10(i)=1/2*atan(2.*Eo_TM_1_10(i).*Eo_TE_1_10(i)*
    cos(delta_fi_out_10)/(Eo_TE_1_10(i).^2-Eo_TM_1_10(i).^2));

    psi_previo2_02(i)=1/2*atan(2.*Eo_TM_2_02(i).*Eo_TE_2_02(i)*
    cos(delta_fi_out_02)/(Eo_TE_2_02(i).^2-Eo_TM_2_02(i).^2));

```

```

psi_previo2_04(i)=1/2*atan(2.*Eo_TM_2_04(i).*Eo_TE_2_04(i)*
cos(delta_fi_out_04)/(Eo_TE_2_04(i).^2-Eo_TM_2_04(i).^2));

psi_previo2_06(i)=1/2*atan(2.*Eo_TM_2_06(i).*Eo_TE_2_06(i)*
cos(delta_fi_out_06)/(Eo_TE_2_06(i).^2-Eo_TM_2_06(i).^2));

psi_previo2_08(i)=1/2*atan(2.*Eo_TM_2_08(i).*Eo_TE_2_08(i)*
cos(delta_fi_out_08)/(Eo_TE_2_08(i).^2-Eo_TM_2_08(i).^2));

psi_previo2_10(i)=1/2*atan(2.*Eo_TM_2_10(i).*Eo_TE_2_10(i)*
cos(delta_fi_out_10)/(Eo_TE_2_10(i).^2-Eo_TM_2_10(i).^2));

end

% All these lines of code, are for avoiding a discontinuity of the
% function tangent in the equation to calculate output polarization angle

difference_1_02=max(psi_previo1_02)-min(psi_previo1_02);
difference_1_04=max(psi_previo1_04)-min(psi_previo1_04);
difference_1_06=max(psi_previo1_06)-min(psi_previo1_06);
difference_1_08=max(psi_previo1_08)-min(psi_previo1_08);
difference_1_10=max(psi_previo1_10)-min(psi_previo1_10);

difference_2_02=max(psi_previo2_02)-min(psi_previo2_02);
difference_2_04=max(psi_previo2_04)-min(psi_previo2_04);
difference_2_06=max(psi_previo2_06)-min(psi_previo2_06);
difference_2_08=max(psi_previo2_08)-min(psi_previo2_08);
difference_2_10=max(psi_previo2_10)-min(psi_previo2_10);

for i=1:1:10000
    if(abs(psi_previo1_02(i+1)-psi_previo1_02(i))>0.5)
        frontera_theta1_02=theta(i+1);
    end
end

for i=1:1:10001
    if(theta(i)>=(frontera_theta1_02))
        psi_1_02(i)=psi_previo1_02(i)+difference_1_02;
    else
        psi_1_02(i)=psi_previo1_02(i);
    end
end

for i=1:1:10000
    if(abs(psi_previo1_04(i+1)-psi_previo1_04(i))>0.5)
        frontera_theta1_04=theta(i+1);
    end
end

for i=1:1:10001
    if(theta(i)>=(frontera_theta1_04))
        psi_1_04(i)=psi_previo1_04(i)+difference_1_04;
    else
        psi_1_04(i)=psi_previo1_04(i);
    end
end

```

```

for i=1:1:10000
    if(abs(psi_previo1_06(i+1)-psi_previo1_06(i))>0.5)
        frontera_theta1_06=theta(i+1);
    end
end

for i=1:1:10001
    if(theta(i)>=(frontera_theta1_06))
        psi_1_06(i)=psi_previo1_06(i)+difference_1_06;
    else
        psi_1_06(i)=psi_previo1_06(i);
    end
end

for i=1:1:10000
    if(abs(psi_previo1_08(i+1)-psi_previo1_08(i))>0.5)
        frontera_theta1_08=theta(i+1);
    end
end
for i=1:1:10001
    if(theta(i)>=(frontera_theta1_08))
        psi_1_08(i)=psi_previo1_08(i)+difference_1_08;
    else
        psi_1_08(i)=psi_previo1_08(i);
    end
end

for i=1:1:10000
    if(abs(psi_previo1_10(i+1)-psi_previo1_10(i))>0.5)
        frontera_theta1_10=theta(i+1);
    end
end

for i=1:1:10001
    if(theta(i)>=(frontera_theta1_10))
        psi_1_10(i)=psi_previo1_10(i)+difference_1_10;
    else
        psi_1_10(i)=psi_previo1_10(i);
    end
end

for i=1:1:10000
    if(abs(psi_previo2_02(i+1)-psi_previo2_02(i))>0.5)
        frontera_theta2_02=theta(i+1);
    end
end
for i=1:1:10001
    if(theta(i)>=(frontera_theta2_02))
        psi_2_02(i)=psi_previo2_02(i)+difference_2_02;
    else
        psi_2_02(i)=psi_previo2_02(i);
    end
end

for i=1:1:10000
    if(abs(psi_previo2_04(i+1)-psi_previo2_04(i))>0.5)
        frontera_theta2_04=theta(i+1);
    end
end

```

```

for i=1:1:10001
    if(theta(i)>=(frontera_theta2_04))
        psi_2_04(i)=psi_previo2_04(i)+difference_2_04;
    else
        psi_2_04(i)=psi_previo2_04(i);
    end
end

for i=1:1:10000
    if(abs(psi_previo2_06(i+1)-psi_previo2_06(i))>0.5)
        frontera_theta2_06=theta(i+1);
    end
end

for i=1:1:10001
    if(theta(i)>=(frontera_theta2_06))
        psi_2_06(i)=psi_previo2_06(i)+difference_2_06;
    else
        psi_2_06(i)=psi_previo2_06(i);
    end
end

for i=1:1:10000
    if(abs(psi_previo2_08(i+1)-psi_previo2_08(i))>0.5)
        frontera_theta2_08=theta(i+1);
    end
end

for i=1:1:10001
    if(theta(i)>=(frontera_theta2_08))
        psi_2_08(i)=psi_previo2_08(i)+difference_2_08;
    else
        psi_2_08(i)=psi_previo2_08(i);
    end
end

for i=1:1:10000
    if(abs(psi_previo2_10(i+1)-psi_previo2_10(i))>0.5)
        frontera_theta2_10=theta(i+1);
    end
end

for i=1:1:10001
    if(theta(i)>=(frontera_theta2_10))
        psi_2_10(i)=psi_previo2_10(i)+difference_2_10;
    else
        psi_2_10(i)=psi_previo2_10(i);
    end
end

dif_ortogonalidad_02=psi_2_02-psi_1_02;
dif_ortogonalidad_04=psi_2_04-psi_1_04;
dif_ortogonalidad_06=psi_2_06-psi_1_06;
dif_ortogonalidad_08=psi_2_08-psi_1_08;
dif_ortogonalidad_10=psi_2_10-psi_1_10;

dif_ortogonalidad_degree_02=dif_ortogonalidad_02*180/pi;
dif_ortogonalidad_degree_04=dif_ortogonalidad_04*180/pi;
dif_ortogonalidad_degree_06=dif_ortogonalidad_06*180/pi;
dif_ortogonalidad_degree_08=dif_ortogonalidad_08*180/pi;
dif_ortogonalidad_degree_10=dif_ortogonalidad_10*180/pi;

```



```
theta_degree=theta*180/pi;

psi_degree1_02=psi_1_02*180/pi;
psi_degree2_02=psi_2_02*180/pi;
psi_degree1_04=psi_1_04*180/pi;
psi_degree2_04=psi_2_04*180/pi;
psi_degree1_06=psi_1_06*180/pi;
psi_degree2_06=psi_2_06*180/pi;
psi_degree1_08=psi_1_08*180/pi;
psi_degree2_08=psi_2_08*180/pi;
psi_degree1_10=psi_1_10*180/pi;
psi_degree2_10=psi_2_10*180/pi;

hold

plot(theta_degree,dif_ortogonalidad_degree_02,'r');
plot(theta_degree,dif_ortogonalidad_degree_04,'g');
plot(theta_degree,dif_ortogonalidad_degree_06,'y');
plot(theta_degree,dif_ortogonalidad_degree_08,'m');
plot(theta_degree,dif_ortogonalidad_degree_10,'b');
title('Output Orthogonality vs input probe power signal')
xlabel('Input polarization orientation');
ylabel('Shift Angle regarding orthogonality');
legend('1 mW', '1.3 mW', '1.6 mW', '1.9 mW', '2.2 mW');
grid
end
%
```

```

function test8

%
%
% Name:      test8.m
%
% Author:    Raúl Martín
%
%
%
% Orthogonality as a function of Input Probe Power for different
% input polarization angles.
%
% variable theta45 contains the angle we want to analyze.
%
%
j=10e7;           % A/m^2      drive current density
q=1.6e-19;       % C          electronic charge
d=0.15e-6;       % m          active layer thickness
a1TE= 2.5e-20;   % m^2        material gain constant
a1TM=2.14e-20;
n0=1.1e24;       % m^-3      transparency carrier density
St=0;            %          average amplified spontaneous
                %          emission
Ts=1e-9;        % s          carrier recombination life
                %          time

w=1.2e-6;
Iprobe_inicial=0.5/(d*w);
St=0;
h=6.6260693e-34; % J*s
v=1.935483e14;  %
E=h*v;

Iprobe02=1e-3/(d*w);
Iprobe04=1.3e-3/(d*w);
Iprobe06=1.55e-3/(d*w);
Iprobe08=1.9e-3/(d*w);
Iprobe10=2.2e-3/(d*w);
Iprobe11=2.5e-3/(d*w);
Idata=1e-3/(d*w);

L=500e-6;        % m          SOA length
landa=1.55e-6;  % m
gammaTE=0.3;     %          Confinement factor TE
gammaTM=0.24;   %          Confinement factor TM
NrTE=3.1;       %          guide refractive index TE
NrTM=2.9;       %          guide refractive index TM
dN=-1.2e-26;    % m^3       Change in refractive index with
                %          carrier density

Iprobe=Iprobe02:(Iprobe11-Iprobe02)/1000:Iprobe11;
theta45=60*pi/180;

% initial value of carrier density to calculate only the relative value
% later, not the absolute value

n_inicial_TE=(j/(q*d)+a1TE*n0*Iprobe_inicial/E+a1TE*n0*Idata/E+a1TE*n0*St)
/(1/Ts+a1TE*Iprobe_inicial/E+a1TE*Idata/E+a1TE*St);

```

```

n_inicial_TM=(j/(q*d)+a1TM*n0*Iprobe_inicial/E+a1TM*n0*Idata/E+a1TM*n0*St)
/(1/Ts+a1TM*Iprobe_inicial/E+a1TM*Idata/E+a1TM*St);

for i=1:1:1001

    % value of carrier concentration for zero input power

    np_TE(i)=(j/(q*d)+a1TE*n0*Iprobe(i)/E+a1TE*n0*St)/(1/Ts+a1TE*
    Iprobe(i)/E+a1TE*St);

    np_TM(i)=(j/(q*d)+a1TM*n0*Iprobe(i)/E+a1TM*n0*St)/(1/Ts+a1TM*
    Iprobe(i)/E+a1TM*St);

    % value of carrier density

    n_TE(i)=(j/(q*d)+a1TE*n0*Idata/E+a1TE*n0*Iprobe(i)/E+a1TE*n0*St)/
    (1/Ts+a1TE*Idata/E+a1TE*Iprobe(i)/E+a1TE*St);

    n_TM(i)=(j/(q*d)+a1TM*n0*Idata/E+a1TM*n0*Iprobe(i)/E+a1TM*n0*St)/
    (1/Ts+a1TM*Idata/E+a1TM*Iprobe(i)/E+a1TM*St);

    % initial phase

    phaseTE_inicial(i)=2*pi*L*(NrTE+gammaTE*np_TE(i)*dN)/landa+2*pi*L*
    gammaTE*(n_inicial_TE-np_TE(i))*dN/landa;

    phaseTM_inicial(i)=2*pi*L*(NrTM+gammaTM*np_TM(i)*dN)/landa+2*pi*L*
    gammaTM*(n_inicial_TM-np_TM(i))*dN/landa;

    % Nonlinear phase change      % Nonlinear phase change

    phaseTE(i)=2*pi*L*(NrTE+gammaTE*np_TE(i)*dN)/landa+2*pi*L*gammaTE*
    (n_TE(i)-np_TE(i))*dN/landa;

    phaseTM(i)=2*pi*L*(NrTM+gammaTM*np_TM(i)*dN)/landa+2*pi*L*gammaTM*
    (n_TM(i)-np_TM(i))*dN/landa;

    % Phase shift along SOA

    phaseTE_shift(i)=phaseTE_inicial(i)-phaseTE(i);
    phaseTM_shift(i)=phaseTM_inicial(i)-phaseTM(i);

    % Phase difference between TM and TE modes

    delta_fi_out(i)=phaseTM_shift(i)-phaseTE_shift(i);

    % Gain for TE and TM modes. Gain ratio

    gain_TE(i)=a1TE*(n_TE(i)-n0);
    gain_TM(i)=a1TM*(n_TM(i)-n0);
    gain_ratio(i)=gain_TE(i)/gain_TM(i);

end

```

```

for i=1:1:1001

    % Eo_TE and Eo_TM as a function of input polarization angle

    Eo_TE_1(i)=(gain_ratio(i).*sqrt(Iprobe(i)).*cos(theta45));
    Eo_TM_1(i)=sqrt(Iprobe(i)).*sin(theta45);

    Eo_TE_2(i)=-gain_ratio(i).*sqrt(Iprobe(i)).*cos(pi/2-theta45);
    Eo_TM_2(i)=sqrt(Iprobe(i)).*sin(pi/2-theta45);

    % output polarization angle

    psi_1(i)=1/2*atan(2.*Eo_TM_1(i).*Eo_TE_1(i)*
    cos(delta_fi_out(i))/(Eo_TE_1(i).^2-Eo_TM_1(i).^2));

    psi_2(i)=1/2*atan(2.*Eo_TM_2(i).*Eo_TE_2(i)*
    cos(delta_fi_out(i))/(Eo_TE_2(i).^2-Eo_TM_2(i).^2));

end

dif_orthogonality=psi_2-psi_1;
dif_orthogonality_degree=dif_orthogonality*180/pi;
psi_degree1=psi_1*180/pi;
psi_degree2=psi_2*180/pi;

Iprobe_jijijuas=Iprobe*d*w*10^3;
plot(Iprobe_jijijuas,dif_orthogonality_degree,'r');
title('Orthogonality for input polarization angle=60°')
xlabel('Input Probe Power');
ylabel('Shift Angle regarding orthogonality');

grid
end

% _____

```